

In presenting the dissertation as a partial fulfillment of the requirements for an advanced degree from the Georgia Institute of Technology, I agree that the Library of the Institute shall make it available for inspection and circulation in accordance with its regulations governing materials of this type. I agree that permission to copy from, or to publish from, this dissertation may be granted by the professor under whose direction it was written, or, in his absence, by the Dean of the Graduate Division when such copying or publication is solely for scholarly purposes and does not involve potential financial gain. It is understood that any copying from, or publication of, this dissertation which involves potential financial gain will not be allowed without written permission.

7/25/68

ANALYSIS OF POOL FILM BOILING

A THESIS

Presented to

The Faculty of the Graduate Division

By

Jean-Claude Moureau

In Partial Fulfillment

of the Requirements for the Degree

Master of Science

in Mechanical Engineering

Georgia Institute of Technology

December, 1972

ANALYSIS
OF
POOL FILM BOILING

Approved: ✓

Chairman, Dr. Novak Zuber

Dr. Stothe P. Kezios

Dr. George M. Rentzepis

Date Approved by Chairman:

Nov. 21, 1972

ACKNOWLEDGMENTS

The author wishes to express his deep appreciation to Professor Novak Zuber for introducing him to the subject, guiding him during all his study and providing him with valuable advice. The author is also indebted to Dr. Zuber for his efforts as chairman of the reading committee and for his review of the manuscript. This gratitude is accompanied by a great admiration for Dr. Zuber's work.

Acknowledgments are also presented to the two other members of the reading committee, Professor S. P. Kezios, Director of the School of Mechanical Engineering, and Professor G. M. Rentzepis for their helpful suggestions and encouragement.

The work presented in this thesis was carried out under sponsorship of the Mechanics Division of the AFOSR Grant No. 70-1853 at the Georgia Institute of Technology. The author wishes to thank the above organization for financial provision for this research.

TABLE OF CONTENTS

	Page
ACKNOWLEDGMENTS	ii
LIST OF ILLUSTRATIONS	iv
NOMENCLATURE	v
SUMMARY	viii
Chapter	
I. INTRODUCTION	1
II. WAVE ANALYSIS	5
2.1 Definition of the Problem	
2.2 Determination of the Potentials	
2.3 Wave Velocity	
III. STABILITY ANALYSIS APPLIED TO FILM BOILING	28
3.1 Rayleigh-Taylor Instability	
3.2 Critical Wavelength	
3.3 Prediction of the Change of Boiling Pattern	
3.4 Most Dangerous Wavelength	
3.5 Most Unstable Disturbance	
IV. DIAMETER AND PERIOD OF BUBBLE RELEASE	51
4.1 Diameter of Bubble at Breakoff	
4.2 Period of Bubble Release	
V. HEAT TRANSFER IN FILM BOILING	59
5.1 Determination of the Minimum Heat Flux	
5.2 Heat Transfer Coefficient in Film Boiling	
VI. CONCLUSION	83
BIBLIOGRAPHY	85

LIST OF ILLUSTRATIONS

Figure	Page
1. Interfacial Wave Between Two Fluids	6
2. Stages in Film Boiling	29
3. Schematic Boiling Pattern	33
4. Schematic Boiling Pattern - Repeated Square	36
5. Model of Film Boiling	66
6. Single Bubble Generating Area	67
7. Heat Transfer Coefficient Versus Temperature Difference for Water	77
8. Heat Flux Versus Temperature Difference for Water	78
9. Heat Transfer Coefficient Versus Temperature Difference for Freon 11	79
10. Heat Flux Versus Temperature Difference for Freon 11	80
11. Heat Transfer Coefficient Versus Temperature Difference for Nitrogen	81
12. Heat Flux Versus Temperature Difference for Nitrogen	82

NOMENCLATURE

Greek Letters

β	growth coefficient
γ	average bubble height
δ	fluid depth
Δ	difference
ϵ	surface emissivity
η'	perturbation
λ	wavelength
μ	viscosity
ν	Lagrangian multiplier
ξ	constant
ρ	density
$\bar{\rho}_1$	density of vapor (see equation (36))
$\bar{\rho}_2$	density of liquid (see equation (36))
σ	surface tension coefficient
Σ	Stefan Boltzmann constant
τ	period of bubble release
ϕ	velocity potential
ψ	Lagrangian multiplier function
ω	wave frequency

Lower Case Letters

a	wave amplitude
f	frequency of bubble release

g	acceleration of gravity
h_c	heat transfer coefficient when radiation is not considered
i	complex number = $\sqrt{-1}$
Δi	heat of vaporization
k	wave number
\dot{m}	mass flow rate
\hat{n}	unit normal vector
n	number of bubbles
q	heat flux
q_c	heat flux when radiation is not considered
r	radial coordinate
t	time
\vec{v}	velocity vector
x	coordinate
y	coordinate
z	coordinate

Capital Letters

D	diameter
G_1	radial vapor flow rate
K	thermal conductivity
M_q	non-dimensional group
N_q	non-dimensional group
P	pressure
R_a	radius of curvature
R_b	radius of curvature

S area
T temperature
 V_1 radial vapor velocity

Subscripts

1 lower fluid (vapor)
2 upper fluid (liquid)
av average
b bubble
c critical
m or max maximum
min minimum
o constant value
r radiative
tot total
w at the wall
x,z components in the x,z directions

Superscripts

. per unit time
' perturbed term
+ non-dimensional group

SUMMARY

The purpose of this thesis is threefold. First, to explain the change of boiling pattern occurring at high pressures in pool film boiling. Secondly, to include in the existing theories of film boiling from horizontal flat surfaces the effect of the mass transfer between the vapor and liquid phases. Thirdly, to extend the usual two-dimensional approach by considering the three-dimensional case.

The stability analysis of waves at the interface of two superposed fluids, known as the Rayleigh-Taylor stability analysis, is modified to take into account the mass transfer between the two heated fluids and their depths. It is shown that the vaporization at the interface has a stabilizing effect on the vapor film. It is concluded that the changes of flow pattern, that is, from vapor bubbles to vapor sheets, which were observed by several investigators of film boiling at high pressures, are due to this stabilizing effect. In particular, this change of flow regime occurs when the vapor thrust number (defined herein) equals unity.

The stability analysis is then used to derive expressions for computing critical and most dangerous wavelengths, bubble breakoff diameters and frequencies of bubble release.

Finally, equations are derived which can be used to determine the minimum heat flux and the heat transfer coefficient in pool film boiling from flat surfaces.

It is shown that all the results predicted by the present

analysis are in good agreement with the experimental data available in the literature.

CHAPTER I

INTRODUCTION

During the last two decades boiling phenomena have received much significant attention. In pool boiling different regimes have been established: nucleate, transition and film boiling. At the present time, each of these regions has been amply described and various models have been presented which correlate satisfactorily most of the experimental results.

However, a number of unsolved problems remain. Among these is the following: in the case of film boiling at high pressure an important change in the flow pattern is observed when the heat flux from the heating surface is increased. At pressures approaching the critical, the thin vapor film covering the surface and from which vapor bubbles are released grows suddenly as the heat flux is increased; a vapor sheet rises and covers the heater, while the regular pattern of bubble release disappears.

Although the photographs of Grigull and Abadzic [1] and Abadzic and Goldstein [2] exhibit very well this variation from the characteristic regularly bubbling vapor film to a large vapor blanket, the reason for this change of flow regime is not known.

One realizes that this vapor sheet occurs at high heat fluxes inducing an important interfacial evaporation. Therefore, it appears that an appropriate analysis of the phenomenon should take the inter-

facial mass transfer effects into account.

Nevertheless, in the literature these effects were not considered or partly neglected.

One of the most often used analysis of film boiling is Zuber's prediction [3] of the minimum heat flux. This derivation is based on the purely hydrodynamic instability of a liquid vapor interface known as the Rayleigh Taylor instability.

The extension of this model to the film boiling region has been done by Berenson [4]. Although he considers a mass flow parallel to the horizontal heating surface and contributing to the growth of the bubbles, Berenson neglects the mass transfer effects when he determines the locations of the prominences which will grow and depart as bubbles; indeed he uses the most unstable wavelength resulting from the Rayleigh Taylor instability analysis. Furthermore, the limits of validity of the predicted film boiling heat transfer coefficient are not well established.

The purpose of this thesis is to introduce the mass transfer terms in a slightly modified Rayleigh Taylor instability analysis in order to explain the change of boiling pattern at high pressure described above. The influence of these interfacial mass transfer terms on the minimum heat flux and the film boiling heat transfer coefficient is also calculated.

Rankin [5] was one of the first to introduce the mass transfer terms into the stability analysis. He concludes that, in the case of vapor below a colder liquid, there is damping of the interfacial wave due to the mass transfer.

As Zuber [6] emphasizes it "Whereas the vaporization at the interface has a destabilizing effect on liquid film, it has a stabilizing effect on vapor film."

In a recent paper, Hsieh [7] arrives at the same conclusion. The application of Hsieh's study to film boiling done by Dhir and Lienhard indicates that, at low pressures, the heat and mass transfer do not influence the flow pattern. However, that work does not give any criterion for the changes of configuration occurring at high pressures which are observed in experiments. Furthermore, it presents a two-dimensional formulation.

As noted by Zuber [3] the two-dimensional approach of the problem was an assumption which should be checked. Hosler and Westwater [8] write that in this problem "a confusing choice of equations arises because of uncertainties in the derivation. Can a two-dimensional model be used or must it be three-dimensional?" Further on the following questions are raised: "Are the bubbles released with a diameter equal to a half wavelength, or is the factor something else? Is the average wavelength the critical value or the most dangerous value? What is the velocity of a bubble leaving the interface?"

In this thesis, a three-dimensional stability analysis of the interface between two fluids of finite depths under the influence of a temperature gradient is presented. A criterion for the change of configuration of film boiling at high pressures is also derived. Then, the results are applied to film boiling from a horizontal flat surface to predict the bubbles diameters at breakoff and their frequency of release. Finally, expressions for the minimum flux and pool film

boiling heat transfer coefficient are obtained.

CHAPTER II

WAVE ANALYSIS

2.1 Definition of the Problem

This analysis will determine the behavior of a flat interface separating two superposed fluids of different densities, subject to the action of small disturbances. The solution of this problem in the two-dimensional approximation can be found in Lamb [9]. The real three-dimensional case has been treated briefly by Maxwell [10].

The model considered is as follows: The underlying fluid (designated by the index 1) has a depth δ_1 measured from a flat plate and a velocity \vec{v}_1 while the upper fluid (index 2) has a depth δ_2 and a velocity \vec{v}_2 . The (x-z) plane is taken as the common boundary of the two undisturbed fluids and the y-axis is directed vertically upwards as shown in Figure 1. For this model, two continuity, two momentum and two energy field equations (one for each fluid), and three jump conditions at the interface are written. This will lead to a general expression of the wave velocity which is introduced in the following chapter into a Rayleigh-Taylor instability analysis applied to pool film boiling.

2.2 Determination of the Potentials

The continuity equations of the two phases reduce for incompressible fluids in irrotational flows to the Laplace's equations:

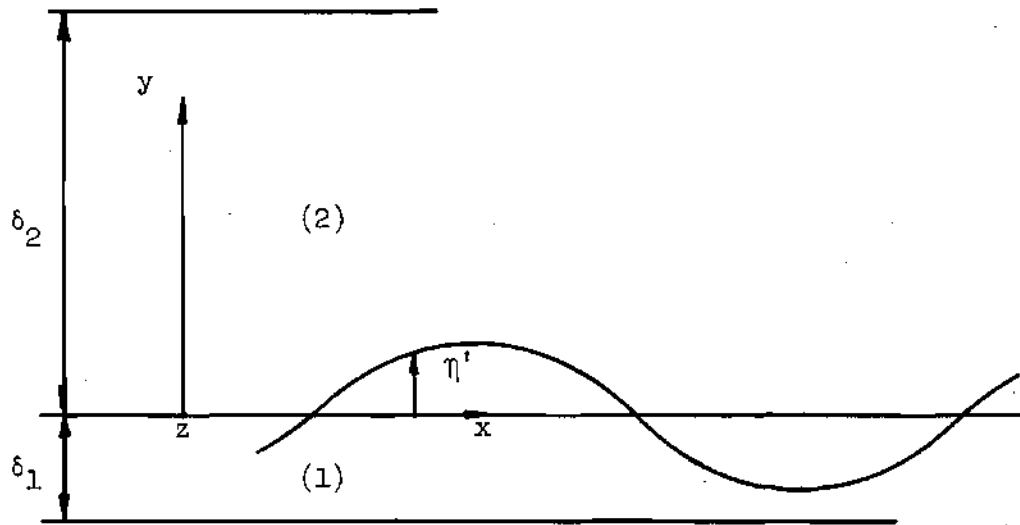


Figure 1. Interfacial Wave Between Two Fluids.

$$\nabla^2 \phi_1 = 0 \quad (1)$$

and

$$\nabla^2 \phi_2 = 0 \quad (2)$$

where ϕ_1 and ϕ_2 are the potentials of the velocities

$$\vec{v}_1 = -\nabla \phi_1 \quad (3)$$

$$\vec{v}_2 = -\nabla \phi_2 \quad (4)$$

It is assumed that irrotational flows exist and the concepts of potential flow theory are used. Some additional restrictions are attached to this presentation; to see these, let us compare the order of magnitude of the various terms of the momentum equation of fluid one (the same could be done for the other fluid)

$$\rho_1 \frac{\partial \vec{v}_1}{\partial t} + \rho_1 \vec{v}_1 \cdot \nabla \vec{v}_1 = -\nabla p_1 + \mu_1 \nabla^2 \vec{v}_1 + \rho_1 \vec{g} \quad (5)$$

When the interface is under the influence of small irregularities it

is displaced and waves are formed. Using the wavelength λ as a scaling factor for the length, ω^{-1} the inverse of the wave frequency for the time and $a\omega$ where a is the amplitude for the velocity, equation (5) becomes

$$\rho_1 a\omega^2 + \rho_1 \frac{a^2 \omega^2}{\lambda} = -\frac{P_1}{\lambda} + \mu_1 \frac{a\omega}{\lambda^2} + \rho_1 g \quad (6)$$

Neglecting the second term of the right hand side before the first term of the left hand side of equation (6) gives:

$$\mu_1 \frac{a\omega}{\lambda^2} \ll \rho_1 a\omega^2$$

or

$$\frac{\rho_1 \lambda^2 \omega}{\mu_1} \gg 1$$

If the effect of viscosity is neglected $\mu_1 \rightarrow 0$, then the above condition is satisfied. Considering the second term of the left hand side of equation (6) small compared to the first gives

$$a\omega^2 \gg \frac{a^2 \omega^2}{\lambda}$$

or

$$a \ll \lambda$$

This states that the amplitude of the wave must be small compared to the wavelength.

The two differential equations (1) and (2) can be solved once the appropriate boundary conditions are specified:

- The two fluids are considered unbounded in the x (positive and negative) and z (positive and negative) directions and their velocities are finite there.

- At $y = -\delta_1$, the y -component of the velocity of the lower fluid is zero

$$v_{1y} = - \frac{\partial \phi_1}{\partial y} \Big|_{y = -\delta_1} = 0 \quad (7)$$

- At $y = +\delta_2$, the y -component of the velocity of the upper fluid is zero

$$v_{2y} = - \frac{\partial \phi_2}{\partial y} \Big|_{y = +\delta_2} = 0 \quad (8)$$

- The conditions at the interface can be found by the following arguments. By definition, the mass of one phase leaving that phase across an interfacial area element is given by Kocamustafaogullari [11]

$$\dot{\hat{n}}_1 = \rho_1 (\vec{v}_1 - \vec{v}_i) \cdot \hat{n}_1$$

and

$$\dot{\hat{n}}_2 = \rho_2 (\vec{v}_2 - \vec{v}_i) \cdot \hat{n}_2$$

where \vec{v}_i denotes the interface velocity and \hat{n}_1 and \hat{n}_2 are the unit normal vectors pointing outwards. If a surface f is given by the equation

$$f(x, y, t) = 0$$

geometric considerations show that

$$\hat{n}_1 = \frac{\nabla f}{|\nabla f|}$$

and

$$\vec{v}_i \cdot \hat{n}_1 = - \frac{\frac{\partial f}{\partial t}}{|\nabla f|}$$

Therefore,

$$\dot{m}_1 = \frac{\rho_1}{|\nabla f|} \left[\vec{v}_1 \cdot \nabla f + \frac{\partial f}{\partial t} \right]$$

or in components

$$\dot{m}_1 = \frac{\rho_1}{|\nabla f|} \left[v_{1x} \frac{\partial f}{\partial x} + v_{1y} \frac{\partial f}{\partial y} + v_{1z} \frac{\partial f}{\partial z} + \frac{\partial f}{\partial t} \right] \quad (9)$$

In this case

$$f = y - \eta'(x, z, t)$$

where $\eta' = \eta'(x, z, t)$ is the equation of the infinitesimal perturbation of the interface and can be written as

$$\eta' = ae^{i(\omega t - k_x x - k_z z)} \quad (10)$$

k_x and k_z being the components of the wave number.

It is noted that

$$\frac{\partial f}{\partial x} = -\frac{\partial \eta'}{\partial x}; \quad \frac{\partial f}{\partial y} = 1; \quad \frac{\partial f}{\partial z} = -\frac{\partial \eta'}{\partial z}; \quad \frac{\partial f}{\partial t} = -\frac{\partial \eta'}{\partial t}$$

Thus equation (9) becomes for fluid one

$$\dot{m}_1 = \frac{\rho_1}{|\nabla f|} \left[-v_{1x} \frac{\partial \eta'}{\partial x} + v_{1y} - v_{1z} \frac{\partial \eta'}{\partial z} - \frac{\partial \eta'}{\partial t} \right] \quad (11)$$

The same type of reasoning leads for the second fluid to

$$\dot{m}_2 = \frac{\rho_2}{|\nabla f|} \left[-v_{2x} \frac{\partial \eta'}{\partial x} + v_{2y} - v_{2z} \frac{\partial \eta'}{\partial z} - \frac{\partial \eta'}{\partial t} \right] \quad (12)$$

Thus, equations (7), (8), (11), and (12) in conjunction with the hypothesis of infinite velocities in the unbounded directions give the necessary boundary conditions to solve equations (1) and (2).

The method of small disturbances may now be applied (see for instance Chandrasekhar [12]). Expressing the velocities in constant and perturbed terms, one obtains

$$v_{1x} = v_{1x0} + v'_{1x} \quad (13)$$

$$v_{1y} = v_{1y0} + v'_{1y} = v'_{1y}$$

$$v_{1z} = v_{1z0} + v'_{1z}$$

$$v_{2x} = v_{2x0} + v'_{2x} \quad (14)^*$$

$$v_{2y} = v_{2y0} + v'_{2y} = v'_{2y}$$

$$v_{2z} = v_{2z0} + v'_{2z}$$

and for the potentials

$$\phi_1 = \phi_{10} + \phi'_1$$

$$\phi_2 = \phi_{20} + \phi'_2$$

The Laplace's equations (1) and (2) for the disturbed parts only become

$$\nabla^2 \phi'_1 = 0 \quad (15)$$

and

$$\nabla^2 \phi'_2 = 0 \quad (16)$$

The corresponding boundary equations can be written as follows (if the

* It is assumed there is no steady component of velocities in the y-direction

second and higher orders in the unsteady parts are neglected): From equations (7) and (8)

$$\text{at } y = -\delta_1, \quad v_{1y}' = \frac{\partial \phi_1'}{\partial y} \Big|_{y=-\delta_1} = 0 \quad (17)$$

$$\text{at } y = +\delta_2, \quad v_{2y}' = \frac{\partial \phi_2'}{\partial y} \Big|_{y=+\delta_2} = 0 \quad (18)$$

The equations (11) and (12) at the interface $y = \eta'$ become

$$\dot{m}_1' = \frac{\rho_1}{|\nabla F|} \left[-v_{1xo}' \frac{\partial \eta'}{\partial x} + v_{1y}' - v_{1zo}' \frac{\partial \eta'}{\partial z} - \frac{\partial \eta'}{\partial t} \right]$$

$$\dot{m}_2' = \frac{\rho_2}{|\nabla F|} \left[-v_{2xo}' \frac{\partial \eta'}{\partial x} + v_{2y}' - v_{2zo}' \frac{\partial \eta'}{\partial z} - \frac{\partial \eta'}{\partial t} \right]$$

It is assumed that during the time of interest, the average film thickness does not change; otherwise, the lower fluid would grow infinitely or vanish completely. Therefore, the mass transfer terms must be set equal to zero and herewith one obtains at $y = \eta'$

$$-v_{1xo}' \frac{\partial \eta'}{\partial x} + v_{1y}' - v_{1zo}' \frac{\partial \eta'}{\partial z} - \frac{\partial \eta'}{\partial t} = 0$$

$$-v_{2xo} \frac{\partial \eta'}{\partial x} + v_{2y}' - v_{2zo} \frac{\partial \eta'}{\partial z} - \frac{\partial \eta'}{\partial t} = 0$$

Since by use of equations (3) and (4),

$$v_{1y}' = - \frac{\partial \phi 1'}{\partial y}$$

$$v_{2y}' = - \frac{\partial \phi 2'}{\partial y}$$

the conditions at $y = \eta'$ become

$$-\frac{\partial \phi 1'}{\partial y} = v_{1xo} \frac{\partial \eta'}{\partial x} + v_{1zo} \frac{\partial \eta'}{\partial z} + \frac{\partial \eta'}{\partial t} \quad (19)$$

$$-\frac{\partial \phi 2'}{\partial y} = v_{2xo} \frac{\partial \eta'}{\partial x} + v_{2zo} \frac{\partial \eta'}{\partial z} + \frac{\partial \eta'}{\partial t} \quad (20)$$

Since η' is not a function of y , one can write

$$\frac{\partial \eta'}{\partial t} \Big|_{y = \eta'} = \frac{\partial \eta'}{\partial t} \Big|_{y = 0}$$

$$\frac{\partial \eta'}{\partial x} \Big|_{y = \eta'} = \frac{\partial \eta'}{\partial x} \Big|_{y = 0}$$

$$\frac{\partial \eta'}{\partial z} \Big|_{y = \eta'} = \frac{\partial \eta'}{\partial z} \Big|_{y = 0}$$

and also subject to the same approximation as before,

$$\frac{\partial \phi_1'}{\partial y} \Big|_{y = \eta'} = \frac{\partial \phi_1'}{\partial y} \Big|_{y = 0}$$

and

$$\frac{\partial \phi_2'}{\partial y} \Big|_{y = \eta'} = \frac{\partial \phi_2'}{\partial y} \Big|_{y = 0}$$

The equations (19) and (20) are therefore valid at $y = 0$. Using the boundary conditions described above one can solve the differential equations (15) and (16) (for instance by using the method of separation of variables) and one gets:

$$\phi_1 = M_1 e^{i(\omega t - k_x x - k_z z)} \frac{e^{k(y+\delta_1)} + e^{-k(y+\delta_1)}}{k[e^{k\delta_1} - e^{-k\delta_1}]} \quad (21)$$

and

$$\phi_2 = M_2 e^{i(\omega t - k_x x - k_z z)} \frac{e^{k(y-\delta_2)} + e^{-k(y-\delta_2)}}{k(e^{k\delta_2} - e^{-k\delta_2})}$$

Where

$$M_1 = -a \left[i\omega - v_{1x0} i k_x - v_{1z0} i k_z \right] \quad (22)$$

$$M_2 = +a \left[i\omega - v_{2x0} i k_x - v_{2z0} i k_z \right]$$

and

$$k = \left[k_x^2 + k_z^2 \right]^{1/2} \quad (23)$$

Note that this result reduces to Lamb's expression [9]

$$\phi_1 = e^{i\omega t} \cosh x \frac{\cosh k(y+\delta_1)}{k \sinh(k\delta_1)} (-a i \omega)$$

if it is assumed that a two-dimensional case exists (no z), that no velocities ($v_{1x0} = 0, v_{1z0} = 0$) exist and that only the cosine part of the exponential e^{ikx} is considered. The justification of not considering the "-i sin k x" part is that it will give, for ω imaginary, an imaginary expression for ϕ_1' and therefore for the velocities.

The equations (21) and (22) allow the complete determination of the velocity field.

2.3 Wave Velocity

The momentum equations for the two incompressible fluids in irrotational motion are given by Milne-Thomson [13].

$$\frac{P_1}{\rho_1} + \frac{1}{2} v_1^2 + gy - \frac{\partial \phi_1}{\partial t} = 0 \quad (24)$$

$$\frac{P_2}{\rho_2} + \frac{1}{2} v_2^2 + gy - \frac{\partial \phi_2}{\partial t} = 0 \quad (25)$$

Using equations (13) and (14), and the linearized approximation

$$\frac{1}{2} v_1^2 = \frac{1}{2} (v_{10} + v_1')^2 = \frac{1}{2} v_{1x0}^2 + v_{1x0} v_{1x}' + \frac{1}{2} v_{1z0}^2 + v_{1z0} v_{1z}'$$

$$\frac{1}{2} v_1^2 = \frac{1}{2} (v_{1x0}^2 + v_{1z0}^2) - v_{1x0} \frac{\partial \phi_1'}{\partial x} - v_{1z0} \frac{\partial \phi_1'}{\partial z}$$

Similarly,

$$\frac{1}{2} v_2^2 = \frac{1}{2}(v_{2x0}^2 + v_{2z0}^2) - v_{2x0} \frac{\partial \phi_2'}{\partial x} - v_{2z0} \frac{\partial \phi_2'}{\partial z}$$

Consequently, the unsteady parts of equations (24) and (25) are written at $y = \eta'$

$$\frac{P_1'}{\rho_1} = \frac{\partial \phi_1'}{\partial t} + v_{1x0} \frac{\partial \phi_1'}{\partial x} + v_{1z0} \frac{\partial \phi_1'}{\partial z} - g\eta' \quad (26)$$

$$\frac{P_2'}{2} = \frac{\partial \phi_2'}{\partial t} + v_{2x0} \frac{\partial \phi_2'}{\partial x} + v_{2z0} \frac{\partial \phi_2'}{\partial z} - g\eta' \quad (27)$$

The interfacial jump condition has been expressed by Kocamustafaogullari [11]

$$P_1 - P_2 + \dot{m}_1 (\vec{v}_1 - \vec{v}_2) \cdot \hat{n}_1 = \sigma \left(\frac{1}{R_a} + \frac{1}{R_b} \right) \quad (28)$$

where σ is the surface tension coefficient and R_a and R_b the radii of curvature.

It is already known that

$$\dot{m}_1 = \rho_1 \vec{v}_1 \cdot \hat{n}_1 - \rho_1 \vec{v}_1 \cdot \hat{n}_1$$

and

$$\dot{m}_2 = \rho_2 \vec{v}_2 \cdot \hat{n}_2 - \rho_1 \vec{v}_1 \cdot \hat{n}_2$$

Since the mass of phase one which leaves phase one across an interfacial area element is equal to the mass of phase two which enters phase two across the same area:

$$\dot{m}_1 + \dot{m}_2 = 0$$

$$-\dot{m}_1 (\rho_1 - \rho_2) = \rho_2 \rho_1 (\vec{v}_1 - \vec{v}_2) \cdot \hat{n}_1$$

or

$$(\vec{v}_1 - \vec{v}_2) \cdot \hat{n}_1 = -\dot{m}_1 \frac{\Delta\rho}{\rho_1 \rho_2}$$

where

$$\Delta\rho = \rho_1 - \rho_2$$

The interfacial condition (28) is then written as:

$$P_1 - P_2 = \dot{m}_1^2 \frac{\Delta\rho}{\rho_1 \rho_2} + \sigma \left(\frac{1}{R_a} + \frac{1}{R_b} \right) \quad (29)$$

The radii of curvature can in their turn be transformed to give approximately:

$$\frac{1}{R_a} = - \frac{\frac{\partial^2 \eta'}{\partial x^2}}{\left[1 + \left(\frac{\partial \eta'}{\partial x} \right)^2 \right]^{3/2}} = - \frac{\partial^2 \eta'}{\partial x^2}$$

and

$$\frac{1}{R_b} = - \frac{\frac{\partial^2 \eta'}{\partial z^2}}{\left[1 + \left(\frac{\partial \eta'}{\partial z} \right)^2 \right]^{3/2}} = - \frac{\partial^2 \eta'}{\partial z^2}$$

Considering again disturbed and undisturbed parts, with

$$\dot{m}_1^2 = (\dot{m}_{10} + \dot{m}'_1)^2$$

the equation (29) gives at $y = \eta'$

$$P_1' - P_2' = 2\dot{m}_{10} \dot{m}_1 \frac{\Delta\rho}{\rho_1\rho_2} - \sigma \left[\frac{\partial^2 \eta'}{\partial x^2} + \frac{\partial^2 \eta'}{\partial z^2} \right] \quad (30)$$

This relation expresses the difference of pressure at the interface and takes into account the surface tension and the mass transfer effects.

How can the mass transfer terms be evaluated? The final purpose is to use this wave analysis for film boiling from a flat plate. In that case of boiling, the lower fluid (Index 1) becomes a vapor phase and the upper fluid (Index 2) a liquid phase. Assuming that the two phases are in thermodynamic equilibrium, from an energy balance we have according to Zuber and Dougherty [15]

$$\dot{m}_1 \Delta i = q_{tot} \quad (31)$$

where Δi is the latent heat of vaporization and q_{tot} the total heat flux from the plate. On the other hand, one can write

$$q_{total} = (h_c + h_r)\Delta T \quad (32)$$

where h_c is the heat transfer coefficient when there is no radiation,

h_r the coefficient of heat transfer by radiation through the lower fluid and ΔT is the temperature difference between the plate and the upper fluid which is assumed at saturation temperature;

$$T_2 = T_{\text{saturation}}$$

Equating (31) and (32) gives

$$\dot{m}_1 = \frac{(h_c + h_r)\Delta T}{\Delta i}$$

or separating as usual

$$\dot{m}_{10} + \dot{m}_1 = \frac{(h_{co} + h_{ro})\Delta T}{\Delta i} + \frac{h_c \Delta T}{\Delta i}$$

It is noted that there is no radiative disturbed term since the temperature is not perturbed. One can thus write

$$\dot{m}_{10} \dot{m}_1 = h_{co} \left(1 + \frac{h_{ro}}{h_{co}}\right) \frac{\Delta T}{\Delta i} \frac{h_c \Delta T}{\Delta i}$$

or

$$\dot{m}_{10} \dot{m}_1 = \left(\frac{h_{co}\Delta T}{\Delta i}\right)^2 \left(1 + \frac{h_{ro}}{h_{co}}\right) \frac{h_c}{h_{co}} \quad (33)$$

By the definition of the conductive heat transfer coefficient, one obtains

$$h_c = \frac{K_1}{\delta_1 + \eta'} = \frac{K_1}{\delta_1 \left(1 + \frac{\eta'}{\delta_1}\right)} = \frac{K_1}{\delta_1} \left(1 - \frac{\eta'}{\delta_1}\right)$$

where again the second and higher orders in η' are neglected and where K_1 is the thermal conductivity of phase one.

Since

$$h_c = h_{co} + h'_c$$

one finds

$$\frac{h'_c}{h_{co}} = -\frac{\eta'}{\delta_1}$$

Introducing this result in equation (33), a final expression for the mass transfer terms is obtained:

$$\dot{m}_{10} \dot{m}_1 = - \left[\frac{h_{co} \Delta T}{\Delta t} \right]^2 \left[1 + \frac{h_{ro}}{h_{co}} \right] \frac{\eta'}{\delta_1} \quad (34)$$

Substituting this into equation (30) leads to the relation of the pressure condition at the interface:

$$P_1' - P_2' = -2 \left[\frac{h_{co} \Delta T}{\Delta f} \right]^2 \left[1 + \frac{h_{ro}}{h_{co}} \right] \rho_1 \rho_2 \frac{\eta'}{\delta_1} - \sigma \left[\frac{\partial^2 \eta'}{\partial x^2} + \frac{\partial^2 \eta'}{\partial z^2} \right] \quad (35)$$

The equations (26), (27), and (35), where the potentials ϕ_1' and ϕ_2' are given by equations (21) and (22) and η' by equation (10) can now be combined to obtain after rearrangement

$$\rho_1 \operatorname{ctnh}(k\delta_1) (\omega - v_{1x0} k_x - v_{1z0} k_z)^2 + \rho_2 \operatorname{ctnh}(k\delta_2) (\omega - v_{2x0} k_x - v_{2z0} k_z)^2 =$$

$$kg\Delta\rho - 2k \left(\frac{h_{co} \Delta T}{\Delta f} \right)^2 \frac{\Delta\rho}{\rho_1 \rho_2} \left(1 + \frac{h_{ro}}{h_{co}} \right) \frac{1}{\delta_1} + \sigma k^3$$

Note that this expression reduces to Lamb's solution [9] in the simplified two dimensional case with unlimited depths and no surface tension nor mass transfer effects.

The solution of this equation for ω gives the frequency equation of the interface which plays, as it will be seen, an important role in the stability analysis

$$\omega = \frac{\bar{\rho}_1 V + \bar{\rho}_2 W \pm \left[-\bar{\rho}_1 \bar{\rho}_2 (V-W)^2 - X(\bar{\rho}_1 + \bar{\rho}_2) \right]^{1/2}}{\bar{\rho}_1 + \bar{\rho}_2} \quad (36)$$

where

$$\bar{\rho}_1 = \rho_1 \operatorname{ctnh}(k\delta_1)$$

$$\bar{\rho}_2 = \rho_2 \operatorname{ctnh}(k\delta_2)$$

$$V = v_{1x0} k_x + v_{1z0} k_z$$

$$W = v_{2x0} k_x + v_{2z0} k_z$$

$$X = 2 \left(\frac{h_{co} \Delta T^2}{\Delta l} \right) \frac{\Delta \rho k}{\rho_1 \rho_2 \delta_1} \left(1 + \frac{h_{ro}}{h_{co}} \right) - kg\Delta\rho - \sigma k^3$$

This expression can be written in terms of the wave velocity c defined by

$$c = \frac{\omega}{k}$$

to obtain the dispersion equation

$$c = \frac{\bar{\rho}_1 \left(\frac{k_x}{k} v_{1xo} + \frac{k_z}{k} v_{1zo} \right) + \bar{\rho}_2 \left(\frac{k_x}{k} v_{2xo} + \frac{k_z}{k} v_{2zo} \right)}{\bar{\rho}_1 + \bar{\rho}_2} \quad (37)$$

$$+ \left\{ \frac{g\Delta\rho}{k(\bar{\rho}_1 + \bar{\rho}_2)} + \frac{\sigma \cdot k}{\bar{\rho}_1 + \bar{\rho}_2} - \frac{2 (h_{co}\Delta T)^2 \Delta\rho}{(\Delta l)^2 \rho_1 \rho_2 (\bar{\rho}_1 + \bar{\rho}_2) k \delta_1} \left(1 + \frac{h_{ro}}{h_{co}} \right) \right.$$

$$\left. - \frac{\rho_1 \rho_2}{(\bar{\rho}_1 \bar{\rho}_2)^2} \left[\left(\frac{k_x}{k} \right) (v_{1xo} - v_{2xo}) + \left(\frac{k_z}{k} \right) (v_{1zo} - v_{2zo}) \right]^2 \right\}^{1/2}$$

It is important to emphasize here that this expression is more general than many other previous results in the fact that it shows the influence on the wave velocity of the limited depths, mean fluid velocities, surface tension and mass transfer effects in a three-dimensional case.

As it was proposed and done by Zuber [3] such wave analysis relations can be used to predict the maximum heat flux as well as the minimum heat flux in pool boiling. In the following parts of this study we shall limit ourselves to the consideration of the minimum heat flux and the pool film boiling region.

CHAPTER III

STABILITY ANALYSIS APPLIED TO FILM BOILING

3.1 Rayleigh-Taylor Instability

In this chapter the Rayleigh-Taylor instability analysis will be applied to pool film boiling, and expressions for the critical wavelength which corresponds to the limit between stable and unstable conditions and for the most dangerous wavelength or the most noticeable wavelength in the unstable region will be derived. These values affect directly the bubbles spacing and size in film boiling.

From various visual observations drawn from Westwater [15], Berenson [4], Nishikawa [16] one can describe the following stages in pool film boiling from a horizontal surface:

Let us start with an approximately flat surface between the vapor and liquid phases (See Figure 2a). Under the action of some perturbation, disturbances of the interface appear; the vapor generated in their vicinity flows toward them and contributes to their growth (see Figure 2b). The protuberances are located in some regular lattice and the distance between them seems more or less constant. They depart from the interface as bubbles and the film becomes flat again (Figure 2c). At locations shifted from a constant quantity new disturbances in the interface are formed (Figure 2d) and depart so that the vapor film is flat again (Figure 2e).

In the Rayleigh-Taylor instability analysis, one assumes that the

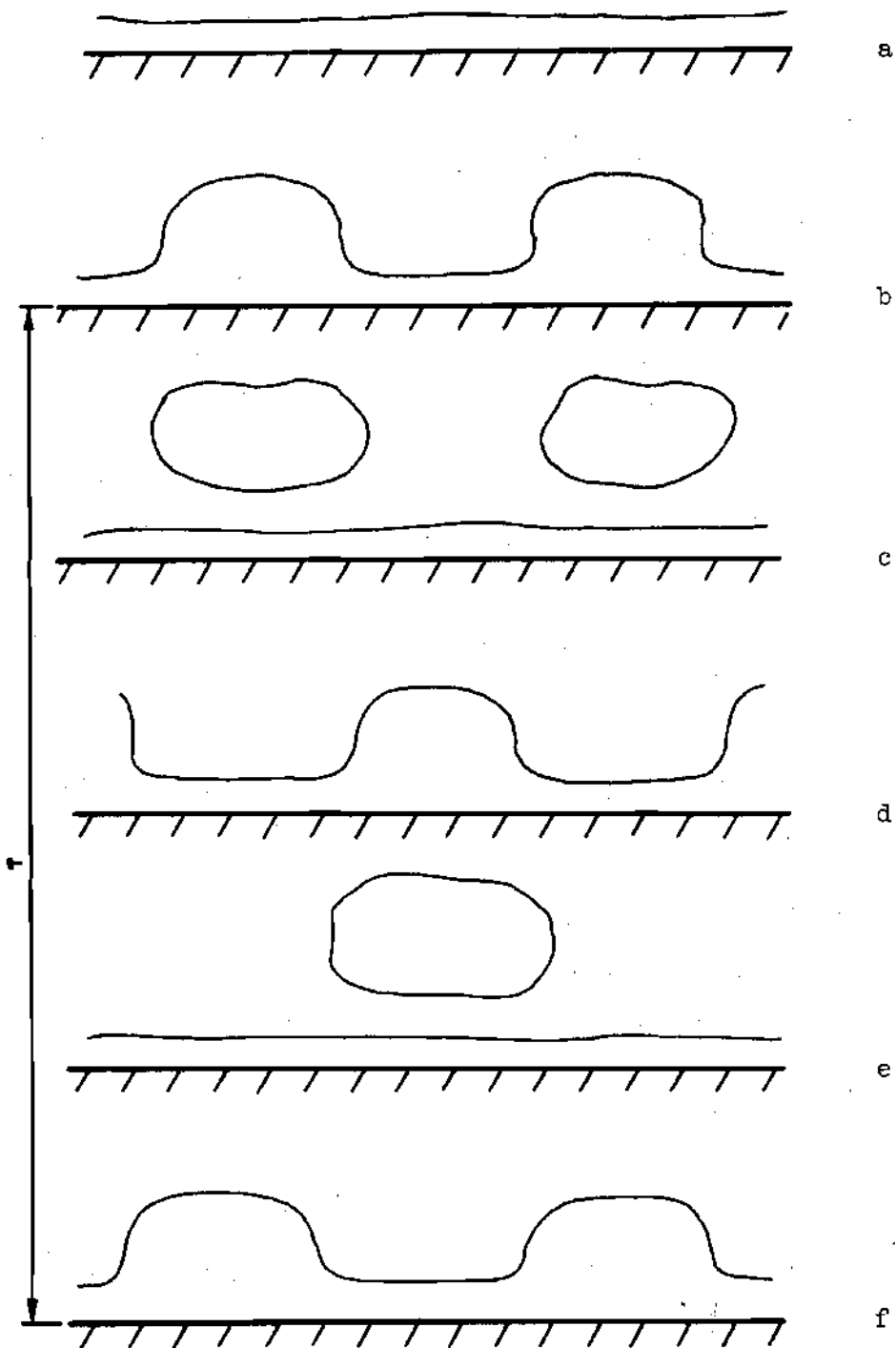


Figure 2. Stages in Film Boiling.

velocities of the two phases are negligible. That means that the mean velocities are equal to zero:

$$v_{1xo} = v_{1zo} = 0$$

$$v_{2xo} = v_{2zo} = 0$$

Is this a reasonable assumption when it is applied to pool film boiling from a horizontal surface?

One seen immediately that since there is no forced convection the velocity of the upper fluid (Index 2) is zero, but it is not evident for the lower fluid. In their discussion of this hypothesis Berenson [4] and Hosler [17] conclude that it is valid near the minimum heat flux but it becomes less accurate when the ΔT is increased. It must be noted that their wave analysis does not take into account the mass transfer terms. The same assumption will be used. The close agreement between the present theory and the experiments shows that even at high ΔT the assumption is reasonable. The general expression of the phase velocity given by equation (37) becomes:

$$c = \frac{\omega}{k} = \pm \left[\frac{g \Delta \rho}{k(\rho_1 + \rho_2)} + \frac{\sigma k}{\rho_1 + \rho_2} - \frac{2(h_{co} \Delta T)^2 \Delta \rho}{(\Delta i)^2 \rho_1 \rho_2 (\rho_1 + \rho_2) k \delta_1} \left(1 + \frac{h_{ro}}{h_{co}}\right) \right]^{1/2}$$

or

$$\omega^2 = \frac{g\Delta\rho k}{\bar{\rho}_1 + \bar{\rho}_2} + \frac{\sigma k^3}{\bar{\rho}_1 + \bar{\rho}_2} - \frac{2(h_{co}\Delta T)^2}{(\Delta l)^2 \rho_1 \rho_2 (\bar{\rho}_1 + \bar{\rho}_2)} \frac{\Delta\rho}{\delta_1} k \left(1 + \frac{h_{ro}}{h_{co}}\right) \quad (38)$$

It is recalled that the perturbation η^* was given by equation (10)

$$\eta^* = ae^{i(\omega t - k_x x - k_z z)} \quad (10)$$

one sees that the sign of ω^2 will determine whether the perturbation will grow or decrease exponentially with time. Thus if ω^2 is negative the interface will be unstable and if ω^2 is positive it will be stable. The condition $\omega^2 = 0$ gives the limit between stability and instability and the corresponding wavenumber is called critical. This limiting case will be discussed first.

3.2 Critical Wavelength

Setting ω^2 given by equation (38) equal to zero and remembering that

$$k^2 = k_x^2 + k_z^2 \quad (23)$$

one obtains

$$k_x^2 + k_z^2 = -\frac{g\Delta\rho}{\sigma} + \frac{2(h_{co}\Delta T)^2}{(\Delta l)^2 \rho_1 \rho_2 \delta_1} \frac{\Delta\rho}{\delta_1} \left(1 + \frac{h_{ro}}{h_{co}}\right) \quad (39)$$

which is a first condition in order to determine the components of the critical wavenumber k_{xc} and k_{zc} . A second condition can be found in the following argument.

Let us consider such a disturbed interface as described above at some fixed time when the bubbles are growing. (See Figure 3 which is a top view). One notices that some pattern is repeated all over the figure.

It has a losenge shape, limited by nodal lines and contains two elevated zones and two depressed. The distance between two crests is λ_x while the distance between the centers of the two depression zones is λ_z . In Figure 3, these distances are not equal and have been chosen arbitrarily. The relation between λ_x and λ_z will now be determined. The surface S of the repeated area is given by

$$S = \frac{2\lambda_x 2\lambda_z}{2} = 2 \lambda_x \lambda_z$$

By the relation between the wavelength and the wavenumber one obtains

$$S = \frac{8\pi^2}{k_x k_z} \quad (39a)$$

The real system adopts the configuration of minimal energy. Since the energy of the wave is directly proportional to its area the system will minimize its area. Therefore, let us minimize the area S given by equation (39a) with the condition expressed by equation (23).

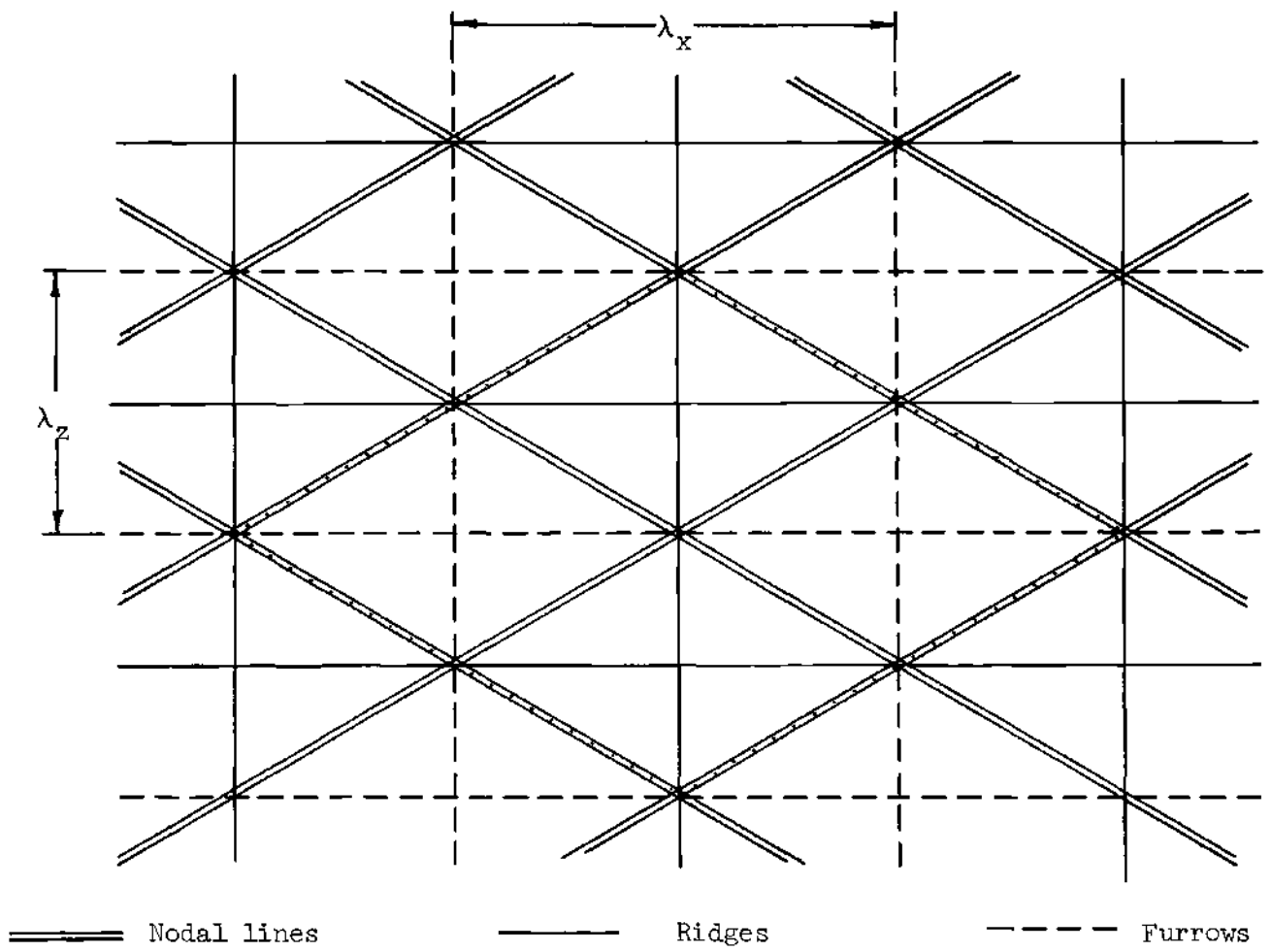


Figure 3. Schematic Boiling Pattern.

Following the Lagrangian multipliers method, the function ψ is defined by

$$\psi = \frac{8\pi^2}{k_x k_z} + v(k_x^2 + k_z^2 - k^2)$$

one then calculates

$$\frac{\partial \psi}{\partial k_x} = -\frac{8\pi^2}{k_x^2 k_z} + 2vk_x = 0$$

$$\frac{\partial \psi}{\partial k_z} = -\frac{8\pi^2}{k_z k_x^2} + 2vk_z = 0$$

$$\frac{\partial \psi}{\partial v} = k_x^2 + k_z^2 - k^2 = 0$$

and obtains

$$v = \frac{4\pi^2}{k_x^3 k_z} = \frac{4\pi^2}{k_z^3 k_x}$$

or

$$k_x^2 = k_z^2 \quad (40)$$

The real pattern is then given by Figure 4 where $\lambda_x = \lambda_z$ and the repeating area is a square. This rejoins Berenson's [24] experimental results: "Visual observations of the bubble pattern which exists on a horizontal surface gave the impression that the bubbles are located in some type of regular lattice, perhaps hexagonal or square."

Combining the condition (39) and (40) gives

$$k_{xc}^2 = k_{zc}^2 = -\frac{g\Delta\rho}{2\sigma} + \frac{(h_{co}\Delta T)^2 \Delta\rho}{(\Delta i)^2 \sigma \rho_1 \rho_2 \delta_1} \left(1 + \frac{h_{ro}}{h_{co}}\right)$$

or in terms of wavelength and since $\Delta\rho = \rho_1 - \rho_2$

$$\lambda_{xc} = \lambda_{zc} = \left[\frac{2\pi}{\frac{g(\rho_2 - \rho_1)}{2\sigma} - \frac{2(h_{co}\Delta T)^2}{(\Delta i)^2 \rho_1 \rho_2 \delta_1 \sigma} \left(1 + \frac{h_{ro}}{h_{co}}\right)} \right]^{1/2} \quad (41)$$

The gravity appears in the denominator of this formula; it has therefore a destabilizing effect which was expected since the lighter phase is below the heavier phase. On the contrary, the surface tension and the mass transfer terms contribute to the stability. One thus arrives at the same conclusions as previous investigators [5,6],[7,11]. Equation (41) can be rewritten as:

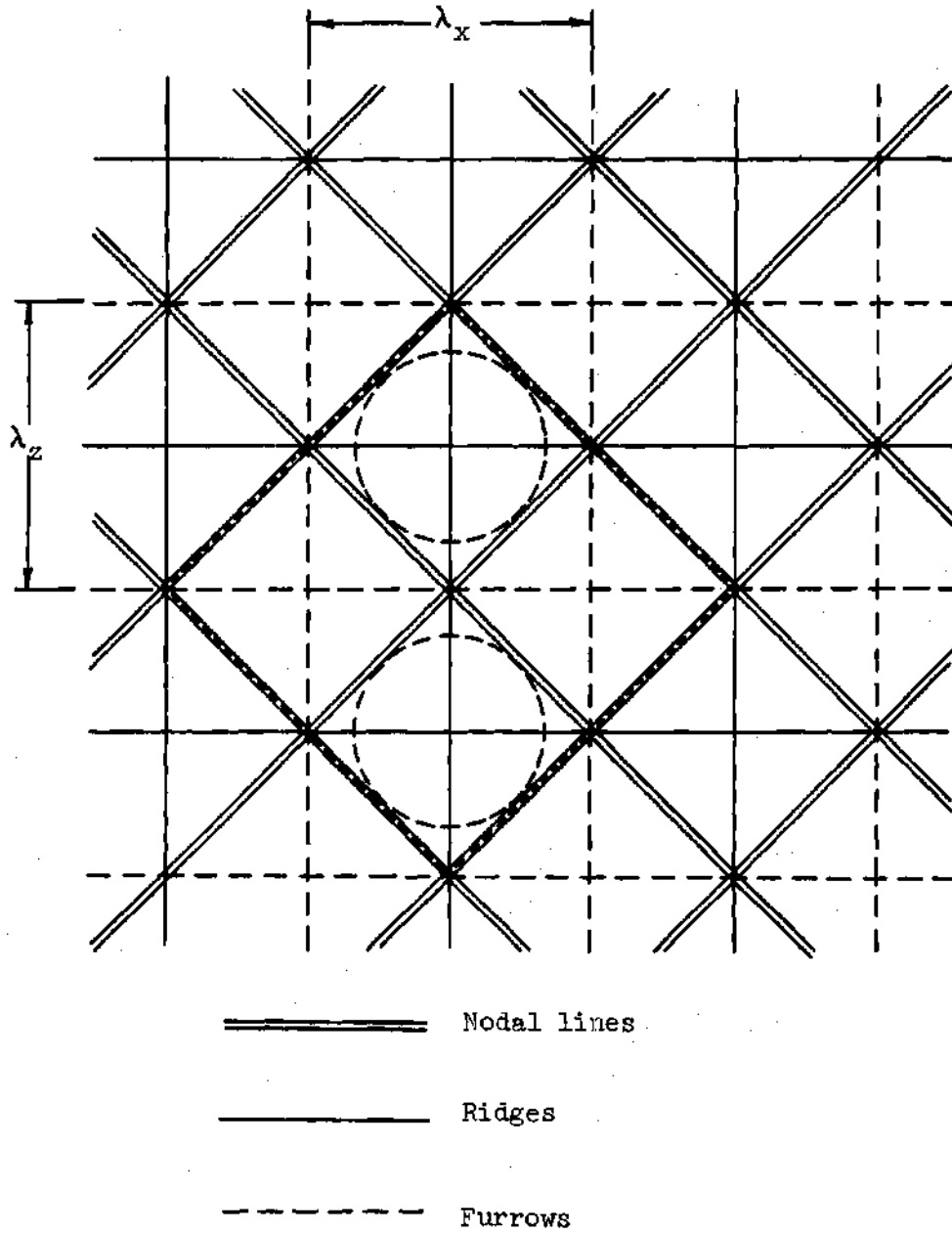


Figure 4. Schematic Boiling Pattern - Repeated Square.

$$\lambda_{xc} = \lambda_{zc} = \frac{2\pi}{\left[\frac{g(\rho_2 - \rho_1)}{2\sigma}\right]^{1/2} \left[1 - \frac{2(h_{co}\Delta T)^2}{(\Delta l)^2 \rho_1 \rho_2 \delta_1 g} \left(1 + \frac{h_{ro}}{h_{co}}\right)\right]^{1/2}} \quad (42)$$

Let us define the vapor thrust number, M_q ,

$$M_q = \frac{2(h_{co}\Delta T)^2}{(\Delta l)^2 \rho_1 \rho_2 \delta_1 g} \left(1 + \frac{h_{ro}}{h_{co}}\right)$$

A non-dimensional group, it is the ratio of the effects of mass transfer and gravity. It may be considered as a kind of Froude number where the inertia forces are replaced by the mass transfer term.

The equation (42) becomes then

$$\lambda_{xc} = \lambda_{zc} = \frac{2\pi}{\left[\frac{g(\rho_2 - \rho_1)}{2\sigma}\right]^{1/2} \left[1 - M_q\right]^{1/2}} \quad (43)$$

or in a non-dimensional form

$$\frac{\lambda_{xc}}{\left[\frac{\sigma}{g(\rho_2 - \rho_1)}\right]^{1/2}} = \frac{\lambda_{zc}}{\left[\frac{\sigma}{g(\rho_2 - \rho_1)}\right]^{1/2}} = \frac{2\sqrt{2}\pi}{\left[1 - M_q\right]^{1/2}} \quad (44)$$

which is the final expression of the critical wavelength. Compare it with Lamb's capillary waves analysis result [9]

$$\lambda = 2\pi \left[\frac{g}{g(\rho_2 - \rho_1)} \right]^{1/2}$$

It is emphasized again that our result is different from the usual purely hydrodynamical Rayleigh-Taylor instability analysis by the presence of the M_q term which accounts for heat transfer effects.

3.3 Prediction of the Change of Boiling Pattern

If the conditions are reached for which the vapor thrust number, M_q , equals unity the critical wavelength becomes infinite. The boiling pattern should then be entirely different. That is exactly what is observed in experiments.

Grigull and Abadzic [1] and also Abadzic and Goldstein [2] have observed film boiling on a wire for conditions close to critical. At low heat flux their photographs show the usual pattern of bubbles leaving regularly the interface. As the heat flux is increased vapor columns are formed, then at some locations vapor sheets rise from the vapor film; and as the heat flux is increased further a vapor sheet covers the entire surface.

The following table summarizes the calculation of M_q for the characteristic example, photographed by Abadzic and Goldstein, of boiling CO_2 (at a pressure of 71.4 bar and a saturation temperature of 29.5°C).

Description of Flow Pattern	q watts/m ²	ΔT °C	M_q
Outset of Formation of Vapor Sheets at Some Locations	1.810^5	200	0.7
Vapor Sheet Covers the Entire Sheet	3.510^5	400	2.88

The observed change of flow pattern at high pressure is thus predicted by the above expressions when the M_q term takes the value of unity. Physically, it means that the effect of the heat flux balances the gravity effect, that is, the vapor thrust is so important that it overcomes the effect of the gravity which tends to bring down the heavy liquid. As M_q increases beyond unity the vapor production is so intense that it becomes a vapor sheet.

At low pressures however, the non-dimensional mass transfer term is generally small. But it increases when one leaves the minimum heat flux and goes further in the film boiling region, i.e., where q and ΔT are increased. The value $M_q = 1$ for Nitrogen at atmospheric pressure is obtained when the heat flux peaks at 1.6510^3 BTU/hr ft² and the temperature difference ΔT at 2.5510^3 °F. At such high conditions the experimental information for boiling from a flat surface is not yet available.

At conditions where the M_q term is larger than one, the present model for film boiling is, of course, no more valid and other theoretical analyses are to be used.

In this section one of the goals of this study has been achieved

that is, a criterion has been derived which predicts the change observed in the flow pattern for vapor bubbles to vapor sheets of film boiling at high pressure.

3.4 Most Dangerous Wavelength

If a disturbance has a wavelength larger than the critical wavelength it will grow exponentially with time. Among all these wavelengths leading to the instability one has the most rapid growth and is therefore called the most dangerous.

From the first section of this chapter it is known that in the unstable region ω^2 is negative. The growth rate of the disturbance $\partial \eta' / \partial t$ is

$$i(\omega t - k_x x - k_z z)$$

$$\frac{\partial \eta'}{\partial t} = i \omega a e$$

The fastest growth rate will thus be obtained by maximizing $(-\omega^2)$. In order to do that, let us calculate:

$$\frac{\partial}{\partial k} (-\omega^2) = 0$$

or with equation (38)

$$\frac{\partial}{\partial k} \left[\frac{2(h_{co} \Delta T)^2 \Delta \rho k}{(\Delta l)^2 \rho_1 \rho_2 (\rho_1^+ \rho_2^-) \delta_1} \left(1 + \frac{h_{ro}}{h_{co}}\right) - \frac{g \Delta \rho k}{\rho_1^+ \rho_2^-} - \frac{\sigma k^3}{\rho_1^+ \rho_2^-} \right] = 0$$

where it is recalled that

$$\overline{\rho}_1 = \rho_1 \operatorname{ctnh}(k\delta_1)$$

$$\overline{\rho}_1 = \rho_2 \operatorname{ctnh}(k\delta_2)$$

one obtains

$$\left[\frac{2(h_{co} \Delta T)^2 \Delta \rho k}{(\Delta l)^2 \delta_1 \rho_1 \rho_2} \left(1 + \frac{h_{ro}}{h_{co}} \right) - g \Delta \rho k - \sigma k^3 \right] \quad (45)$$

$$\left[\rho_1 \delta_1 \operatorname{csch}^2(k\delta_1) + \rho_2 \delta_2 \operatorname{csch}^2(k\delta_2) \right] +$$

$$+ \left[\frac{2(h_{co} \Delta T) \Delta \rho}{(\Delta l)^2 \delta_1 \rho_1 \rho_2} - g \Delta \rho - 3\sigma k^2 \right]$$

$$\left[\rho_1 \operatorname{ctnh}(k\delta_1) + \rho_2 \operatorname{ctnh}(k\delta_2) \right] = 0$$

It will be noted that this expression reduces to the result previously found by Bankoff [18], if we omit the mass transfer term; (there is a misprint in equation (6) of this reference: k must multiply the first term of the numerator).

In film boiling the depth of the liquid phase is generally large and the vapor film is very thin. It is therefore assumed that

$$k\delta_2 \gg 1$$

and

$$k\delta_1 \ll 1$$

This is an improvement in regard to the frequent assumption of two infinitely deep fluids. Therefore,

$$\bar{\rho}_2 = \rho_2 \operatorname{ctnh}(k\delta_2) \approx \rho_2$$

$$\rho_2 \delta_2 \operatorname{csch}^2(k\delta_2) \approx \rho_2 \delta_2 \frac{1}{k^2 \delta_2^2} = \frac{\rho_2}{k^2 \delta_2} \approx 0$$

while for phase one

(+): But the derivation of the most dangerous wavelength made in a subsequent paper by Kesselring and Alii [19] is incorrect.

$$\bar{\rho}_1 = \rho_1 \operatorname{ctnh}(k\delta_1) = \frac{1}{k\delta_1}$$

$$\rho_1 \delta_1 \operatorname{csch}^2(k\delta_1) = \frac{\rho_1}{k^2 \delta_1}$$

The condition (45) takes then a simplified form:

$$\left[\frac{2(h_{co} \Delta T)^2 \Delta \rho}{(\Delta i)^2 \delta_1 \rho_1 \rho_2} k \left(1 + \frac{h_{ro}}{h_{co}}\right) - g \Delta \rho k - \sigma k^3 \right] \left[\frac{\rho_1}{k^2 \delta_1} \right] + \quad (46)$$

$$\left[\frac{2(h_{co} \Delta T)^2 \Delta \rho}{\delta_1 \rho_1 \rho_2} \left(1 + \frac{h_{ro}}{h_{co}}\right) - g \Delta \rho - 3\sigma k^2 \right] \left[\frac{\rho_1}{k \delta_1} + \rho_2 \right] = 0$$

Rearranged in terms of the non-dimensional group M_q this expression is a third order equation in k .

$$2 M_q - 2 + \delta_1 \frac{\rho_2}{\rho_1} (M_q - 1)k + 4 \frac{\sigma}{g(\rho_2 - \rho_1)} k^2 + 3\delta_1 \frac{\rho_2}{\rho_1} \frac{\sigma}{g(\rho_2 - \rho_1)} k^3 = 0$$

Introducing a non-dimensional expression for k

$$k^+ = k\delta_1$$

This third order equation takes a non-dimensional form

$$2 M_q - 2 + \left(\frac{\rho_2}{\rho_1}\right) (M_q - 1) k^+ + 4 \frac{\sigma}{g(\rho_2 - \rho_1) \delta_1^2} k^{+2} \quad (47)$$

$$+ 3 \left(\frac{\rho_2}{\rho_1}\right) \frac{\sigma}{g(\rho_2 - \rho_1) \delta_1^2} k^{+3} = 0$$

This expression gives the correct k allowing to find the most dangerous wavelength. Since it is not very easy to handle, a simplified equation which in many cases leads to a result approaching closely the exact result is proposed.

Notice that equation (45) can be written again as:

$$-3\sigma k^2 \left[\frac{\frac{4}{3} \frac{\rho_1}{k\delta_1} + \rho_2}{2 \frac{\rho_1}{k\delta_1} + \rho_2} \right] - g\Delta\rho + \frac{2(h_{co}\Delta T)^2 \Delta\rho}{(\Delta l)^2 \rho_1 \rho_2 \delta_1} \left(1 + \frac{h_{ro}}{h_{co}}\right) = 0$$

If the factor in brackets in the first term is nearly unity one can approximate this relation by

$$3\sigma k^2 = \frac{2(h_{co}\Delta T)^2 \Delta\rho}{(\Delta l)^2 \delta_1 \rho_1 \rho_2} \left(1 + \frac{h_{ro}}{h_{co}}\right) - g\Delta\rho$$

or with non-dimensional groups

$$k^{+2} = \frac{1}{3} \left[\frac{g(\rho_2 - \rho_1)\delta_1^2}{\sigma} \right] \left[1 - Mq \right] \quad (48)$$

The results of the exact and of the approximate equations are compared for four different fluids in film boiling conditions: water, freon 11, n-pentane, carbon tetrachloride. The following table summarizes the results.

Type of Fluids	Heat Flux q Btu/hr ft ²	Temperature Difference ΔT °F	k^+ equation (47)	k^+ equation (48)
Water	$1.1 \cdot 10^4$	$2.85 \cdot 10^2$	$3.31 \cdot 10^{-2}$	$3.27 \cdot 10^{-2}$
Freon 11	$5.7 \cdot 10^3$	$1.6 \cdot 10^2$	$2.72 \cdot 10^{-2}$	$2.45 \cdot 10^{-2}$
N-Pentane	$7.7 \cdot 10^3$	$2.06 \cdot 10^2$	$4.33 \cdot 10^{-2}$	$4.07 \cdot 10^{-2}$
Carbon Tetrachloride	$6.75 \cdot 10^3$	$1.93 \cdot 10^2$	$3.09 \cdot 10^{-2}$	$2.86 \cdot 10^{-2}$

The difference between the values of the k^+ 's is so small that one can reasonably use equation (48).

Remembering that equations (23) and (40) give

$$k^2 = k_x^2 + k_z^2 = 2k_x^2 = 2k_z^2 \quad (49)$$

the components of the most dangerous wavenumber are found

$$k_{xm} = k_{zm} = \left[-\frac{g\Delta\rho}{6\sigma} + \frac{2(h_{co}\Delta T)^2}{6(\Delta i)^2 \sigma \rho_1 \rho_2 \delta_1} \left(1 + \frac{h_{ro}}{h_{co}}\right) \right]^{1/2} \quad (50)$$

or in terms of wavelength

$$\lambda_{xm} = \lambda_{zm} = \frac{2\pi}{\left[\frac{g(\rho_2 - \rho_1)}{6\sigma} - \frac{2(h_{co}\Delta T)^2(\rho_2 - \rho_1)}{(\Delta i)^2 6\sigma \rho_1 \rho_2 \delta_1} \left(1 + \frac{h_{ro}}{h_{co}}\right) \right]^{1/2}}$$

which becomes with non-dimensional groups

$$\lambda_{xm} = \lambda_{zm} = \frac{2\pi}{\left[\frac{g(\rho_2 - \rho_1)}{6\sigma} \right]^{1/2} \left[1 - M_q \right]^{1/2}} \quad (51)$$

or

$$\frac{\lambda_{xm}}{\left[\frac{\sigma}{g(\rho_2 - \rho_1)}\right]^{1/2}} = \frac{\lambda_{zm}}{\left[\frac{\sigma}{g(\rho_2 - \rho_1)}\right]^{1/2}} = \frac{2\sqrt{6} \pi}{\left[1 - M_q\right]^{1/2}} \quad (52)$$

This relation gives thus the components of the most dangerous wavelength, i.e., the wavelength which corresponds to the maximum growth rate of the disturbance. The effect of our three-dimensional analysis is noted in the factor $2\sqrt{6}$. Indeed, a factor $2\sqrt{3}$ was obtained in the two-dimensional formulation. Another difference with this last approach is, of course, the presence of the M_q term. By comparison of equations (44) and (52) it is interesting to note that

$$\lambda_{xm} = \lambda_{zm} = \sqrt{3} \lambda_{xc} = \sqrt{3} \lambda_{zc}$$

It has thus been shown in this chapter that the liquid vapor interface in film boiling is unstable when the wavelength is larger than the critical wavelength given by equation (44) and stable otherwise. In contrast to gravity, the surface tension and mass transfer have a stabilizing action. Equation (52) constitutes the expression of the wavelength which will be the most dangerous since it leads to the biggest and thus most noticeable growth rate.

3.5 Most Unstable Disturbance

The maximized expression of $(-w^2)$ can now be obtained by introducing in it the most dangerous wavenumber.

Equation (38) is combined with equations (49) and (50) to yield the following result

$$-w^2 = \frac{2}{3} \left[\frac{g(\rho_2 - \rho_1)}{\bar{\rho}_1 + \bar{\rho}_2} - \frac{2(h_{co} \Delta T)^2 (\rho_2 - \rho_1)}{(\Delta i)^2 \rho_1 \rho_2 (\bar{\rho}_1 + \bar{\rho}_2) \delta_1} \left(1 + \frac{h_{ro}}{h_{co}}\right) \right] x$$

$$\left[\frac{g(\rho_2 \rho_1)}{3\sigma} - \frac{2(h_{co} \Delta T)^2}{3(\Delta i)^2 \sigma \rho_1 \rho_2 \delta_1} \left(1 + \frac{h_{ro}}{h_{co}}\right) \right]^{1/2}$$

The most unstable disturbance η_m^* is thus obtained from this equation and equation (10)

$$\beta t = ik_{xm} x - ik_{zm} z \quad (53)$$

$$\eta_m^* = a e$$

where the growth coefficient β is given by:

$$\beta = \left[\frac{2g(\rho_2 - \rho_1)}{3(\bar{\rho}_1 + \bar{\rho}_2)} - \frac{4(h_{co} \Delta T)^2 (\rho_2 - \rho_1)}{3(\Delta l)^2 \rho_1 \rho_2 (\bar{\rho}_1 + \bar{\rho}_2) \delta_1} \left(1 + \frac{h_{ro}}{h_{co}}\right) \right]^{1/2}$$

$$\left[\frac{g(\rho_2 - \rho_1)}{3\sigma} - \frac{2(h_{co} \Delta T)^2 (\rho_2 - \rho_1)}{3(\Delta l)^2 \sigma \rho_1 \rho_2 \delta_1} \right]^{1/4}$$

It is possible to rewrite this with the help of the usual dimensionless group:

$$\beta = \frac{2^{1/2}}{3^{3/4}} \frac{1}{(\bar{\rho}_1 + \bar{\rho}_2)^{1/2}} \left[\frac{g(\rho_2 - \rho_1)}{\sigma} \right]^{1/2} \left[\frac{g(\rho_2 - \rho_1)}{\sigma} \right]^{1/4} \left[1 - M_q \right]^{3/4}$$

In this relation $\bar{\rho}_1$ and $\bar{\rho}_2$ are still functions of the wavenumber and have also to be replaced by their appropriate values determined from the previous hypothesis concerning the depths of the two phases

$$\bar{\rho}_2 = \rho_2$$

and

$$\bar{\rho}_1 = \frac{\rho_1}{k\delta_1}$$

Introducing in this last expression the most dangerous wavenumber leads to

$$\beta = \frac{2^{1/2}}{3} \left[\frac{g(\rho_2 - \rho_1)}{\rho_1} \right]^{1/2} \left[\frac{g(\rho_2 - \rho_1)}{\sigma} \right]^{1/4} \left[\frac{g(\rho_2 - \rho_1) l^2}{\sigma} \right]^{1/4} \left[\frac{1 - M_q}{1 + \frac{1}{\sqrt{3}} \frac{\rho_2}{\rho_1} \left[\frac{g(\rho_2 - \rho_1) \delta_1^2}{\sigma} \right]^{1/2} \left[1 - M_q \right]^{1/2}} \right]^{1/2} \quad (54)$$

This expression gives thus the growth coefficient (which has the dimension of the inverse of a time) for the most unstable disturbance. One observes the effects on this relation of the three-dimensional analysis by the coefficients, of the vapor depth by the factor δ_1^2 and of the mass transfer by the presence of M_q .

Another evidence for the validity of the analysis is shown by equation (54). Note that when the vapor thrust number M_q approaches unity the growth coefficient β approaches zero. Therefore, since β has the dimension of the inverse of a time, that is, of frequency, the period of oscillations tends to infinity. The phenomenon ceases to be periodic both in time and in space. The covering vapor sheet results in a stable boiling pattern.

CHAPTER IV

DIAMETER AND PERIOD OF BUBBLE RELEASE

4.1 Diameter of Bubble at Breakoff

The disturbances created on the interface grow in shape of approximately spherical bubbles whose diameters at breakoff and frequency of release will be the next subject of investigation.

In the Figure 4 which represents a projection of the liquid vapor interface on a horizontal surface, one may consider one of the repeated squares. As described before, two bubbles are formed and grow simultaneously in such an area. Westwater and Santangelo [15] observed that the bubble breaks at the nodal lines. Therefore, the shape of the bubble is idealized by a sphere whose diameter D_b is given by the length of the side of the square on the nodal lines

$$D_b^2 = \left(\frac{\lambda_x}{2}\right)^2 + \left(\frac{\lambda_z}{2}\right)^2 = 2\left(\frac{\lambda_x}{2}\right)^2 = 2\left(\frac{\lambda_z}{2}\right)^2 = \frac{\lambda_x^2}{2} = \frac{\lambda_z^2}{2}$$

or

$$D_b = \frac{\lambda_x}{\sqrt{2}} = \frac{\lambda_z}{\sqrt{2}} \quad (55)$$

where the wavelength components λ_x and λ_z in the spectrum

$$\lambda_{xc} = \lambda_{zc} < \lambda_x = \lambda_z < \lambda_{xm} = \lambda_{zm} \quad (56)$$

are taken following the method discussed by Zuber [3]. Combining equation (55) with equation (43) and (51) leads to

$$\frac{2\pi}{\left[\frac{g(\rho_2 - \rho_1)}{\sigma}\right]^{1/2} [1 - M_q]^{1/2}} \leq D_b \leq \frac{2\pi\sqrt{3}}{\left[\frac{g(\rho_2 - \rho_1)}{\sigma}\right]^{1/2} [1 - M_q]^{1/2}}$$

which can be rearranged in a non-dimensional form:

$$\frac{2\pi}{[1 - M_q]^{1/2}} \leq D_b^+ \leq \frac{2\pi\sqrt{3}}{[1 - M_q]^{1/2}} \quad (57)$$

where the dimensionless diameter of the bubble at breakoff is

$$D_b^+ = \frac{D_b}{\left[\frac{\sigma}{g(\rho_2 - \rho_1)}\right]^{1/2}} \quad (58)$$

It is interesting to compare this result with the expressions most often used in the literature.

In his original two-dimensional analysis Zuber [3] found

$$\pi \leq D_b^+ \leq \sqrt{3} \pi$$

On the other hand, Berenson [4] determined from experiments of film boiling on a horizontal surface

$$D_b^+ = 4.7$$

From stability characteristics of the neck surface which connects the bubble to the interface Kiper [20] proposed a maximum bubble size given by

$$D_b^+ = 9.28$$

Lienhard and Wong [21] have shown that the heater geometry affects the diameter of the bubble at breakoff: the results being different if it is a flat plate, a large or a small wire. The present analysis concerns film boiling from a flat plate. Only a few experiments have been carried out and reported for that geometry.

Hosler and Westwater [8] data concerning mainly the minimum heat flux region are probably among the most important of these. They use water and freon 11 in their experiments; as they point it out these two

fluids have very different physical properties and constitute "a severe test for any theoretical or empirical expression for boiling."

The comparison between our expression of D_b^+ and their measurements at the minimum heat flux conditions is therefore presented in the following table

	Analysis		Experiments [8]			
	M_q	D_b^+ min.	D_b^+ max.	D_b^+ avg.	D_b^+ min.	D_b^+ max.
Water	$8 \cdot 10^{-4}$	6.28	10.88	7.49	5.97	9.41
Freon 11	$5.8 \cdot 10^{-3}$	6.3	10.91	8.31	6.56	10.28

In both cases we notice that the dimensionless term M_q is very small and its effect on D_b^+ is nearly negligible. However, it is not always the case, as it is known from the previous chapter.

4.2 Period of Bubble Release

As in the beginning of this chapter, let us consider a single bubble generating area, and call τ the time which elapses between the formation of two bubbles on the same location (See Figure 2). The frequency of bubble release is the inverse of this time, i.e.,

$$f = \frac{1}{\tau}$$

From the figure it is seen that the time it takes for the boundary to grow one height equal to the bubble diameter is

$$t = \frac{\tau}{4}$$

But also by definition

$$t = \frac{D_b}{\frac{\partial \eta}{\partial t}}$$

Consequently the frequency is given by

$$f = \frac{1}{4} \frac{\partial \eta}{\partial t} \frac{1}{D_b} \quad (59)$$

The value of D_b is already known; how can $\partial \eta / \partial t$ be evaluated?

From equation (53)

$$\frac{\partial \eta}{\partial t} = \beta \eta$$

From his experimental observations Lewis [22] noted that the amplitude of the wave increases exponentially until it reaches a maximum value approximately equal to 0.4 times the wavelength. It will be noted here that this value is considerably less restrictive than the assumption of the linearized theory

$$a \ll \lambda$$

Since η^* varies from an infinitesimal value to that upper limit a mean value for the growth rate can be used:

$$\overline{\frac{\partial \eta^*}{\partial t}} = \beta \frac{0.4 \lambda_x}{2} = 0.2 \beta \lambda_x \quad (60)$$

The equation (59) can then be transformed:

$$f = 0.05 \beta \lambda_x \frac{1}{D_b}$$

Replacing D_b by its expression given by equation (55) yields to

$$f = 0.05\sqrt{2} \beta$$

The value of the growth coefficient has been determined by equation (54). By substitution one finds:

$$f = \frac{0.033 \left[\frac{g(\rho_2 - \rho_1)}{\rho_1} \right]^{1/2} \left[\frac{g(\rho_2 - \rho_1)}{\sigma} \right]^{1/4} \left[\frac{g(\rho_2 - \rho_1) \delta_1^2}{\sigma} \right]^{1/4} [1 - M_q]}{\left\{ 1 + \frac{1}{\sqrt{3}} \frac{\rho_2}{\rho_1} \left[\frac{g(\rho_2 - \rho_1) \delta_1^2}{\sigma} \right]^{1/2} [1 - M_q]^{1/2} \right\}^{1/2}}$$

This frequency of bubble release can be rewritten in a non-dimensional form.

$$f^+ = \frac{0.033 \left[\frac{g(\rho_2 - \rho_1) \delta_1^2}{\sigma} \right]^{1/4} [1 - M_q]}{\left\{ 1 + \frac{1}{\sqrt{3}} \frac{\rho_2}{\rho_1} \left[\frac{g(\rho_2 - \rho_1) \delta_1^2}{\sigma} \right]^{1/2} [1 - M_q]^{1/2} \right\}^{1/2}}$$

where the dimensionless frequency f^+ is defined by:

$$f^+ = \frac{f}{\left[\frac{g(\rho_2 - \rho_1)}{\rho_1} \right]^{1/2} \left[\frac{g(\rho_2 - \rho_1)}{\sigma} \right]^{1/4}}$$

The comparison between this frequency of bubble release and the measurements of Hosler and Westwater is presented in the following table. The calculations have been performed for the inverse of the non-dimensional bubble frequency the dimensionless period τ^+ and for the same fluids and conditions as in the previous section.

Analysis	Experiments [8]		
	τ^+	τ^+ avg.	τ^+ min. τ^+ max.
Water	$5.92 \cdot 10^2$	$5.52 \cdot 10^2$	$3.03 \cdot 10^2$ $8.55 \cdot 10^2$
Freon 11	$2.41 \cdot 10^2$	$2.7 \cdot 10^2$	$1.27 \cdot 10^2$ $4.125 \cdot 10^2$

One sees immediately the good agreement between the theory and the experiments. Furthermore, from the previous estimation of the bubble diameter it is known that the M_q term is small for such conditions near the minimum heat flux at atmospheric pressure; therefore, it does not affect considerably the expressions of the period calculated above. It should however become more important at high heat fluxes and pressures. Experimental verification of this on horizontal flat surfaces is badly needed.

CHAPTER V

HEAT TRANSFER IN FILM BOILING

5.1 Determination of the Minimum Heat Flux

This chapter is related to two specific heat transfer subjects: the prediction of the minimum heat flux and the determination of the heat transfer coefficient in pool film boiling. Two different approaches are used. The first one which follows Zuber's model is presented next while the second based on Berenson's film boiling analysis is discussed in the following section.

Let's assume that the flat horizontal surface on which the film boiling takes place has an area ab ; first n , the number of bubbles released per unit time in that area, will be evaluated.

Consider in Figure 4 which represents the flow pattern one of the repeating squares of area $2\lambda_x^2$. It contains four bubble generating locations. (Indeed, as described before, in half a period two bubbles grow simultaneously in the square and after another half period two other bubbles have grown in shifted positions; which makes a total of four). The number of bubbles n is thus the product of the number of squares in the area of interest ab by four times the frequency of bubble release

$$n = \frac{ab}{2\lambda_x^2} \cdot 4 \cdot f$$

The frequency to be used for the determination of the minimum heat flux is, following the method of Zuber [3], the frequency obtained by the interface stability analysis and given by equation (59). This substitution gives:

$$n = \frac{ab}{2\lambda_x} \cdot 4 \cdot \frac{1}{4} \frac{\partial \eta'}{\partial t} \frac{1}{D_b}$$

which can in turn be combined with the value already obtained for D_b in equation (55) to yield

$$n = \frac{ab}{\sqrt{2}} \frac{1}{\lambda_x^3} \frac{\partial \eta'}{\partial t}$$

Therefore, the number of bubbles released per unit time and unit area is

$$n = \frac{1}{\sqrt{2}} \frac{1}{\lambda_x^3} \frac{\partial \eta'}{\partial t} \quad (62)$$

On the other hand, the vapor flow rate per unit area carried away by the assumed spherical bubbles is

$$\dot{m}_1' = \rho_1 \cdot \frac{4\pi}{3} \left(\frac{\lambda_x}{2\sqrt{2}} \right)^3 \cdot n$$

or after rearrangement with equation (62)

$$\dot{m}_1 = \rho_1 \frac{\pi}{24} \frac{\partial \eta'}{\partial t}$$

The energy balance of equation (31) gives the expression of the minimum heat flux

$$q_{\min} = \dot{m}_1 \Delta i = \rho_1 \frac{\pi}{24} \frac{\partial \eta'}{\partial t} \Delta i$$

Substituting $\partial \eta' / \partial t$ by its value given by equation (60) where β and λ_x are replaced by their expressions as given in equations (56) and (51) leads to

$$0.110 \frac{\left[\frac{g(\rho_2 - \rho_1)}{\rho_1} \right]^{1/2} \left[\frac{g(\rho_2 - \rho_1) \delta_1^2}{\sigma} \right]^{1/4} \left[1 - M_q \right]^{1/2}}{\left[\frac{g(\rho_2 - \rho_1)}{\sigma} \right]^{1/4} \left\{ 1 + \frac{1}{\sqrt{3}} \frac{\rho_2}{\rho_1} \left[\frac{g(\rho_2 - \rho_1) \delta_1^2}{\sigma} \right]^{1/2} \left[1 - M_q \right]^{1/2} \right\}^{1/2}}$$

$$\leq q_{\min} \leq$$

$$0.190 \frac{\left[\frac{g(\rho_2 - \rho_1)}{\rho_1} \right]^{1/2} \left[\frac{g(\rho_2 - \rho_1) \delta_1^2}{\sigma} \right]^{1/4} \left[1 - M_q \right]^{1/2}}{\left[\frac{g(\rho_2 - \rho_1)}{\sigma} \right]^{1/4} \left\{ 1 + \frac{1}{\sqrt{3}} \frac{\rho_2}{\rho_1} \left[\frac{g(\rho_2 - \rho_1) \delta_1^2}{\sigma} \right]^{1/2} \left[1 - M_q \right]^{1/2} \right\}^{1/2}}$$

This two limiting expressions of the minimum heat flux in pool film boiling can be rewritten in a non-dimensional form

$$\frac{0.110 \left[1 - M_q \right]^{1/2} \left[1 + \frac{\rho_2}{\rho_1} \right]^{1/2}}{\left\{ \frac{1}{\sqrt{3}} \frac{\rho_2}{\rho_1} \left[1 - M_q \right]^{1/2} + \left[\frac{\sigma}{g(\rho_2 - \rho_1) \delta_1^2} \right]^{1/2} \right\}^{1/2}} \leq q_{\min}^+ \leq (63)$$

$$\frac{0.190 \left[1 - M_q \right]^{1/2} \left[1 + \frac{\rho_2}{\rho_1} \right]^{1/2}}{\left\{ \frac{1}{\sqrt{3}} \frac{\rho_2}{\rho_1} \left[1 - M_q \right]^{1/2} + \left[\frac{\sigma}{g(\rho_2 - \rho_1) \delta_1^2} \right]^{1/2} \right\}^{1/2}}$$

where q_{\min}^+ the dimensionless minimum heat flux is defined by

$$q_{\min}^+ = \frac{q}{\rho_1 \Delta t \left[\frac{\sigma g (\rho_2 - \rho_1)}{(\rho_1 + \rho_2)^2} \right]^{1/4}}$$

a usual group in the literature.

These analytical expressions are once more compared with Hosler and Westwater [8] experiments of boiling from a flat aluminum heating surface 8 inches square; the following table is obtained where the agreement is satisfactory

	Analysis	Experiments [8]
Water	$0.143 \leq q_{\min}^+ \leq 0.247$	$q_{\min}^+ \approx 0.206$
Freon 11	$0.135 \leq q_{\min}^+ \leq 0.234$	$q_{\min}^+ \approx 0.194$

It is emphasized above that the influence of the M_q term on the diameter at breakoff and on the frequency of bubble release is not very appreciable for low heat fluxes and temperature differences at atmospheric pressure. The same holds of course for the determination of the minimum heat flux itself.

From experiments of film boiling of n-pentane and carbon tetrachloride, Berenson [4] measured

$$q_{\min}^+ = 0.09$$

Hosler and Westwater [8] explain this rather low value by the use of a too small heating horizontal surface: "Since the interbubble distance expected in film boiling with ordinary liquids is in the order of one inch, there may be a significant edge effect with a surface only two inch diameter."

Varying his assumptions concerning the bubble velocity at breakoff, the relation between diameter and wavelength or the flow pattern, Zuber

[3,23] has proposed different expressions of the minimum heat flux:

$$q^+ = 0.130 \quad (64a)$$

$$q^+ = 0.099 \quad (64b)$$

$$q^+ = 0.176 \quad (64c)$$

$$q^+ = 0.193 \quad (64d)$$

$$q^+ = 0.013 \quad (64e)$$

Both the present analysis and the experimental results noted above show that equations (64c) and (64d) are to be recommended for film boiling from a flat surface. A fact known by many experimentators is also recognized: the results of Zuber's two-dimensional analysis although independent of thermal transport properties yield to acceptable values of the minimum heat flux at low pressures.

5.2 Heat Transfer Coefficient in Film Boiling

In this section Berenson's model [24] for the determination of the heat transfer coefficient in film boiling is modified by introducing in it the results of the previous wave stability analysis. This will give an expression of this coefficient valid not only in the vicinity of the minimum heat flux but also much higher in the film

boiling region.

The purpose is to evaluate the thickness δ_1 of the vapor film from which the heat transfer coefficient is immediately deduced.

A part of the vapor produced at the interface compensates the decrease of the film thickness between the bubble domes. Therefore, there, the film thickness δ_1 is approximately constant. Another part of the vapor produced flows towards these domes to contribute to their growth and finally their departure as bubbles.

A representation similar to Berenson's model is adopted (See Figure 5). The vapor velocity V_1 is assumed parallel to the flat heating surface and directed in the radial direction. The system exhibits a cylindrical symmetry. (See also Figure 6). The vapor flow rate flowing radially G_1 is given by

$$G_1 = \rho_1 V_1 2\pi r \delta_1 \quad (65)$$

In the following equations the heat transfer by radiation through the vapor film will not be considered. In other words, only one of the part of the total heat flux q_{tot} of equation (32) is examined:

$$q_c = h_c \Delta T = q_{tot} - q_r \quad (66)$$

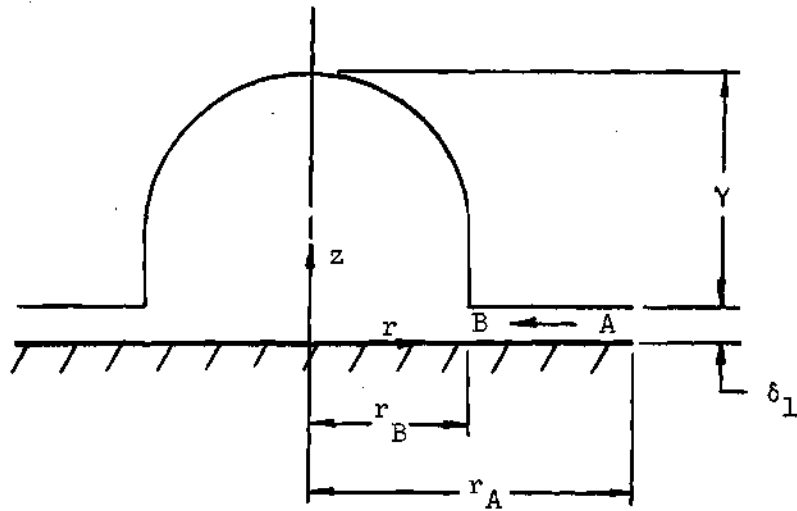


Figure 5. Model of Film Boiling.

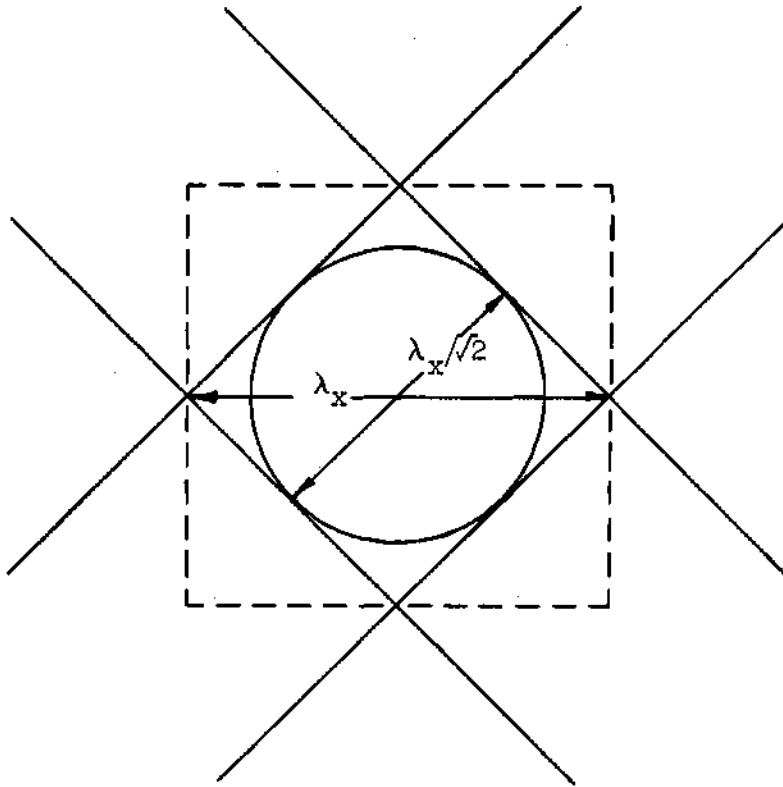


Figure 6. Single Bubble Generating Area.

The radiative contribution q_r to the total heat flux from the surface can be in a first approach determined by [25],

$$q_r = \epsilon \Sigma (T_w^4 - T_2^4) \quad (67)$$

where ϵ is the heated surface emissivity and Σ the Stefan Boltzmann constant.

This elimination of the radiative heat transfer effect leads to introduce a dimensionless group other than the M_q term which was defined by

$$M_q = \frac{2(h_c \Delta T)^2}{(\Delta i)^2 \rho_1 \rho_2 \delta_1 g} \left(1 + \frac{h_r}{h_c}\right)$$

Let this new non-dimensional group N_q be given by:

$$N_q = \frac{2(h_c \Delta T)^2}{(\Delta i)^2 \rho_1 \rho_2 \delta_1 g} \quad (68)$$

which is exempt of radiative term and which will be used in the following derivation. Note for further use the relation:

$$N_q = \frac{M_q}{\left(1 + \frac{h_r}{h_c}\right)} \quad (69)$$

The amount of heat passing through the vapor film is thus (Figure 5)

$$\frac{K_1}{\delta_1} \Delta T (\pi r_A^2 - \pi r^2)$$

which is equal to

$$G_1 \Delta i$$

where Δi is the average enthalpy difference between vapor and liquid. Equating these two expressions where G_1 has been replaced by its value from equation (65) gives the vapor velocity in the flat film

$$v_1 = \frac{K_1 \Delta T (\pi r_A^2 - \pi r^2)}{\rho_1 (\Delta i) \delta_1^2}$$

Considering the three-dimensional flow pattern (Figure 6) one sees that the vapor generated in an area equal to λ_x^2 flows into one bubble, therefore

$$\pi r_A^2 = \lambda_x^2$$

Replacing in the above expression of the velocity, one obtains

$$v_1 = \frac{K_1 \Delta T (\lambda_x^2 - \pi r^2)}{\rho_1 (\Delta l) \delta_1^2} \quad (70)$$

If the momentum forces are neglected before the viscous forces, the momentum equation can be written in the same way as Bromley [26] did

$$\frac{dP}{dr} = \frac{\xi \mu_1 v_1}{\delta_1^2}$$

where ξ is a constant whose value will be determined later.

Introducing the value of the vapor velocity determined in equation (70) into this expression yields to

$$\frac{dP}{dr} = \frac{\xi \mu_1 K_1 \Delta T (\lambda_x^2 - \pi r^2)}{\rho_1 (\Delta l) \delta_1^4 2\pi r}$$

This relation can be integrated between position A (at radius r_A and pressure P_A) and position B (at the radius r_B and pressure P_B), making use of a value of r_B equal to the one-half bubble diameter which is given by equation (55)

$$r_B = \frac{1}{2} D_b = \frac{\lambda_x}{2\sqrt{2}}$$

to obtain

$$P_A - P_B = \frac{0.081}{\pi} \frac{\epsilon \mu_1 K_1 T}{\rho_1 \delta_1^4 (\Delta t)} \lambda_x^2 \quad (71)$$

It is now assumed that the appropriate wavelength λ_x can be obtained from the previous results of the stability analysis applied to film boiling and that it is legitimate to replace λ_x by its maximum value λ_{xm} the most dangerous wavelength. From equation (51)

$$\lambda_{xm}^2 = \frac{24 \pi^2 \sigma}{g(\rho_1 - \rho_2) [1 - N_q]} \quad (72)$$

Combining equations (71) and (72) gives

$$P_A - P_B = \frac{6.107 \epsilon \mu_1 K_1 \Delta T \sigma}{\rho_1 (\Delta t) \delta_1^4 g(\rho_2 - \rho_1) (1 - N_q)}$$

It is possible to evaluate this pressure difference by another means. Let P_o be the pressure at a height γ above the vapor film. The difference of pressure between P_A and P_o will be equal to $\gamma \rho_2 g$ plus a term due to the difference of pressure at the interface. This same last term will be present in the difference of pressure between P_B and P_o which contains also $\gamma \rho_1 g + \frac{2\sigma}{D_{b/2}}$.

Therefore

$$P_A - P_B = \gamma \rho_2 g - \gamma \rho_1 g - \frac{2\sigma}{D_b} \quad (74)$$

Borishansky cited by Berenson [24] measured γ to be

$$\gamma = 0.68 D_b \quad (75)$$

If D_b is replaced as above by $(\lambda_{xm})/(\sqrt{2})$, combining equations (51), (74), and (75) one obtains

$$P_A - P_B = \frac{g(\rho_2 - \rho_1) [65.76 - 3.26 (1 - N_q)]}{8.88 \left[\frac{g(\rho_2 - \rho_1)}{\sigma} \right]^{1/2} [1 - N_q]} \quad (76)$$

Equating equations (76) and (73) and solving for δ_1 yields to

$$\delta_1 = \left\{ \frac{54.3 \epsilon \mu_1 K_1 \Delta T \sqrt{\sigma}}{[65.76 - 3.26 (1 - N_q)] [1 - N_q]^{1/2} \rho_1 \Delta i g(\rho_2 - \rho_1) \sqrt{g(\rho_2 - \rho_1)}} \right\}^{1/4}$$

The fact that only a part of the surface area is covered by a film of constant thickness must now be taken into account, and following Berenson's method the equation above is multiplied by the ratio of the total surface area to the area between the bubbles. Considering

Figure 6 this ratio is seen to be equal to two which yields to

$$\delta_1 = \left\{ \frac{870 \xi}{\left[65.76 - 3.26 (1 - N_q) \right] \left[1 - N_q \right]^{1/2}} \frac{\mu_1 K_1 \Delta T \sqrt{\sigma}}{\rho_1 \Delta l \ g (\rho_2 - \rho_1) \sqrt{g (\rho_2 - \rho_1)}} \right\}^{1/4} \quad (77)$$

Since by definition

$$q = h_c \Delta T = \frac{K_1}{\delta_1} \Delta T$$

the heat transfer coefficient h_c is given by the following expression

$$h_c = \left\{ \frac{\left[65.76 - 3.26 (1 - N_q) \right] \left[1 - N_q \right]^{1/2} K_1^3 \rho_1 \Delta l \ g (\rho_2 - \rho_1)}{870 \xi \mu_1 \Delta T \sqrt{\frac{\sigma}{g (\rho_2 - \rho_1)}}} \right\}^{1/4} \quad (78)$$

where ξ must still be determined, which is done as follows. This heat transfer coefficient although derived for the film boiling region must also be valid at the minimum heat flux where it takes the value of $h_{c \min}$. On the other hand, we can calculate a heat transfer coefficient $h_{c \min}$ from our theoretical expression of q_{\min} , given by equation (63), by:

$$h_{c \min} = \frac{q_{\min}}{\Delta T}$$

Applying this to water and equating the two gives a numerical value of ξ which can then be introduced in equation (78) to yield:

$$h_c = \frac{\left\{ [65.76 - 3.26 (1 - N_q)^{1/2}] [1 - N_q] \right\}^{1/4}}{5.417} \left\{ \frac{K_1^3 \rho_1 \Delta i g (\rho_2 - \rho_1)}{\mu_1 \Delta T \sqrt{\frac{\sigma}{g (\rho_2 - \rho_1)}}} \right\}^{1/4} \quad (79)$$

This final expression of the heat transfer coefficient in the film boiling region can be expressed in a non-dimensional form:

$$h_c^+ = \frac{\left\{ [65.76 - 3.26 (1 - N_q)^{1/2}] [1 - N_q] \right\}^{1/2}}{5.417} \quad (80)$$

where h_c^+ the dimensionless heat transfer coefficient is obtained by

$$h_c^+ = \frac{h_c}{\left\{ \frac{K_1^3 \rho_1 \Delta i g (\rho_2 - \rho_1)}{\mu_1 \Delta T \sqrt{\frac{\sigma}{g (\rho_2 - \rho_1)}}} \right\}^{1/4}}$$

In equation (79) or (80), due to its exponent, the N_q term does not affect very much the value of the heat transfer coefficient as long as N_q is much smaller than unity. As it becomes comparable to one (which can be realized at high pressures or extremely high heat fluxes),

it contributes to decrease the heat transfer coefficient which is in concordance with the experimental results of Abadzic and Goldstein [2]. Furthermore, the value of unity for N_q which would cancel the expression of the heat transfer coefficient is not acceptable. Indeed our model is limited to the case where M_q equals one (See Chapter III, Section 3). Therefore, by equation (69), N_q cannot reach the value of unity without being outside of the domain of validity of the expressions.

This analytical result for the heat transfer coefficient is now compared with the experiments of Hosler and Westwater [8] at atmospheric pressure in the vicinity of the minimum heat flux (moderate ΔT).

Nature of Fluid	ΔT (°F)	h_c^+ From Analysis	h_c^+ From Experiments [8]
Water	285	0.519	0.56
Water	345	0.519	0.55
Water	385	0.519	0.54
Freon 11	220	0.519	0.53
Freon 11	280	0.519	0.5
Freon 11	375	0.517	0.5

The good agreement between the theory and the experiments can be seen. This is confirmed at higher heat fluxes and temperature differ-

ence as it is shown in the following table.

Sauer and Ragsdell [27] performed experiments of film boiling of nitrogen on a flat horizontal two inches heater. They obtained data for temperature differences as high as 1250°F where there is a radiative contribution to the total heat flux. By deducing this contribution from their measurements they propose results where the radiation is not included which is exactly what is done in this analysis of the heat transfer coefficient h_c . The comparison is thus adequate and presented here

Nature of Fluid	ΔT (°F)	h_c^+ From Analysis	h_c^+ From Experiments [27]
Nitrogen	500	0.51	0.52
Nitrogen	200	0.504	0.49
Nitrogen	1250	0.489	0.47

In Figures 7 to 12 the above comparisons are expressed in terms of dimensional heat fluxes and heat transfer coefficients.

In all the instances the agreement between the theory and the experiments is seen to be good, and therefore the proposed heat transfer coefficient is recommended for pool film boiling on horizontal flat surfaces.

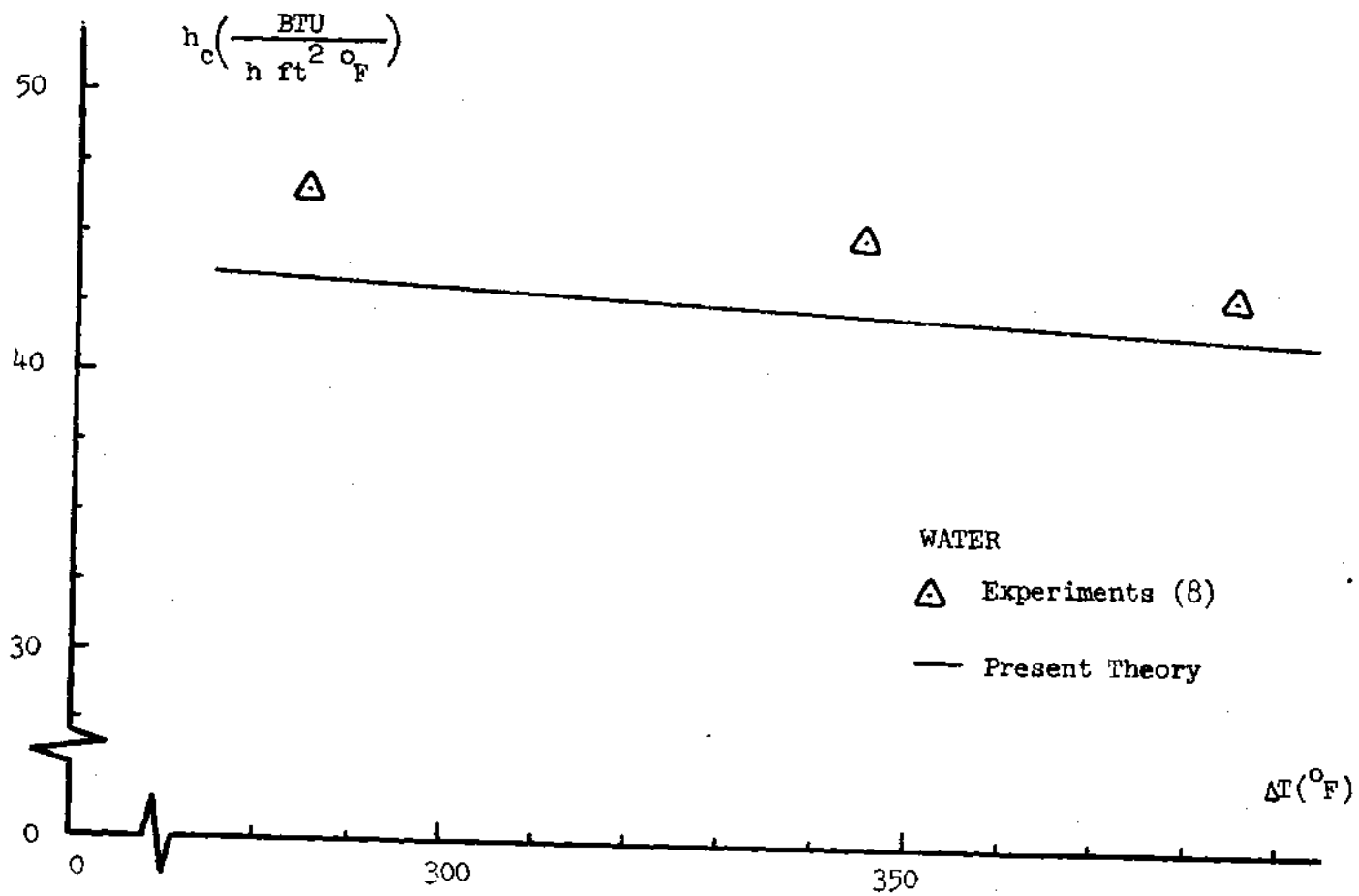


Figure 7. Heat Transfer Coefficient Versus Temperature Difference for Water.

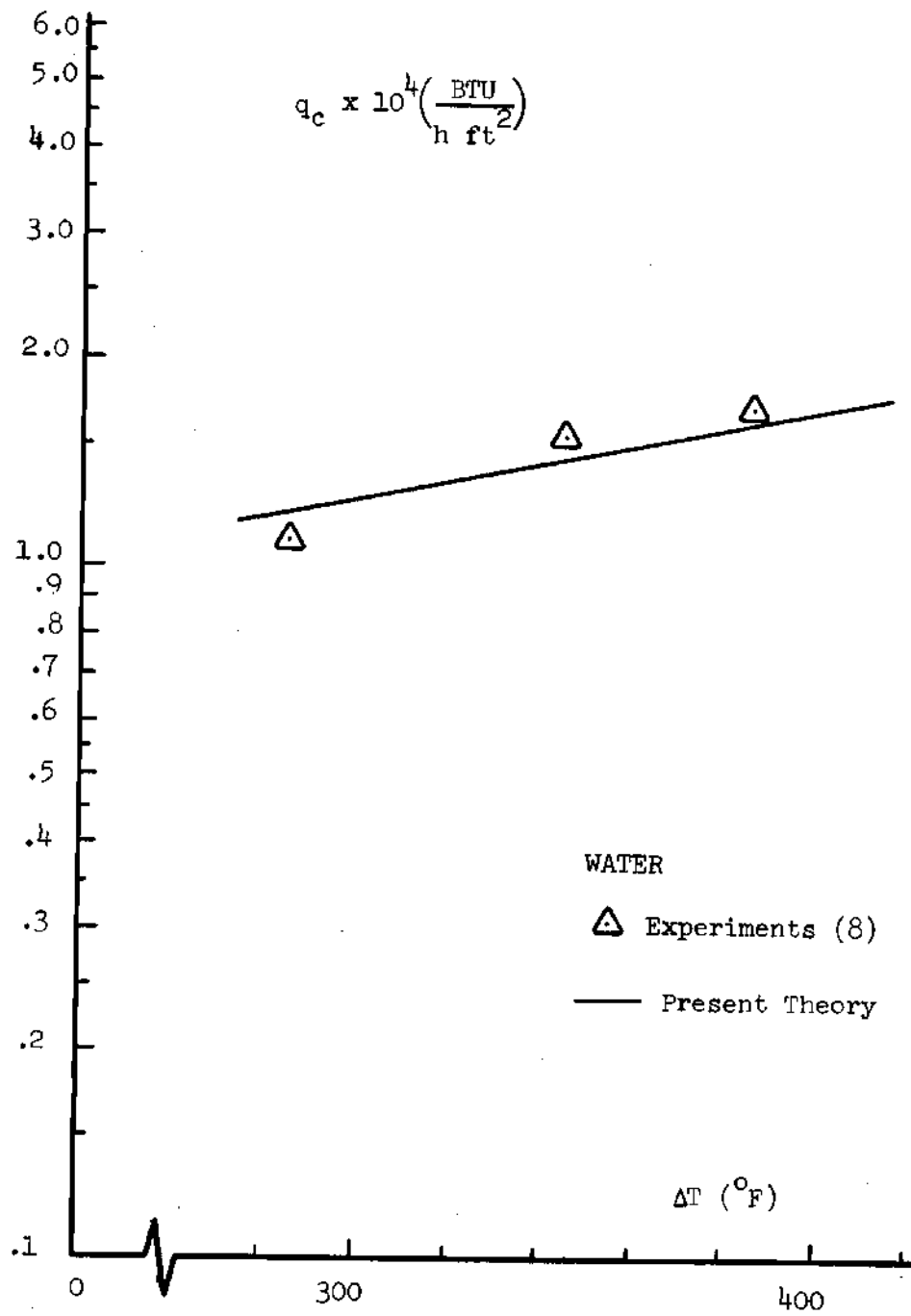


Figure 8. Heat Flux Versus Temperature Difference for Water.

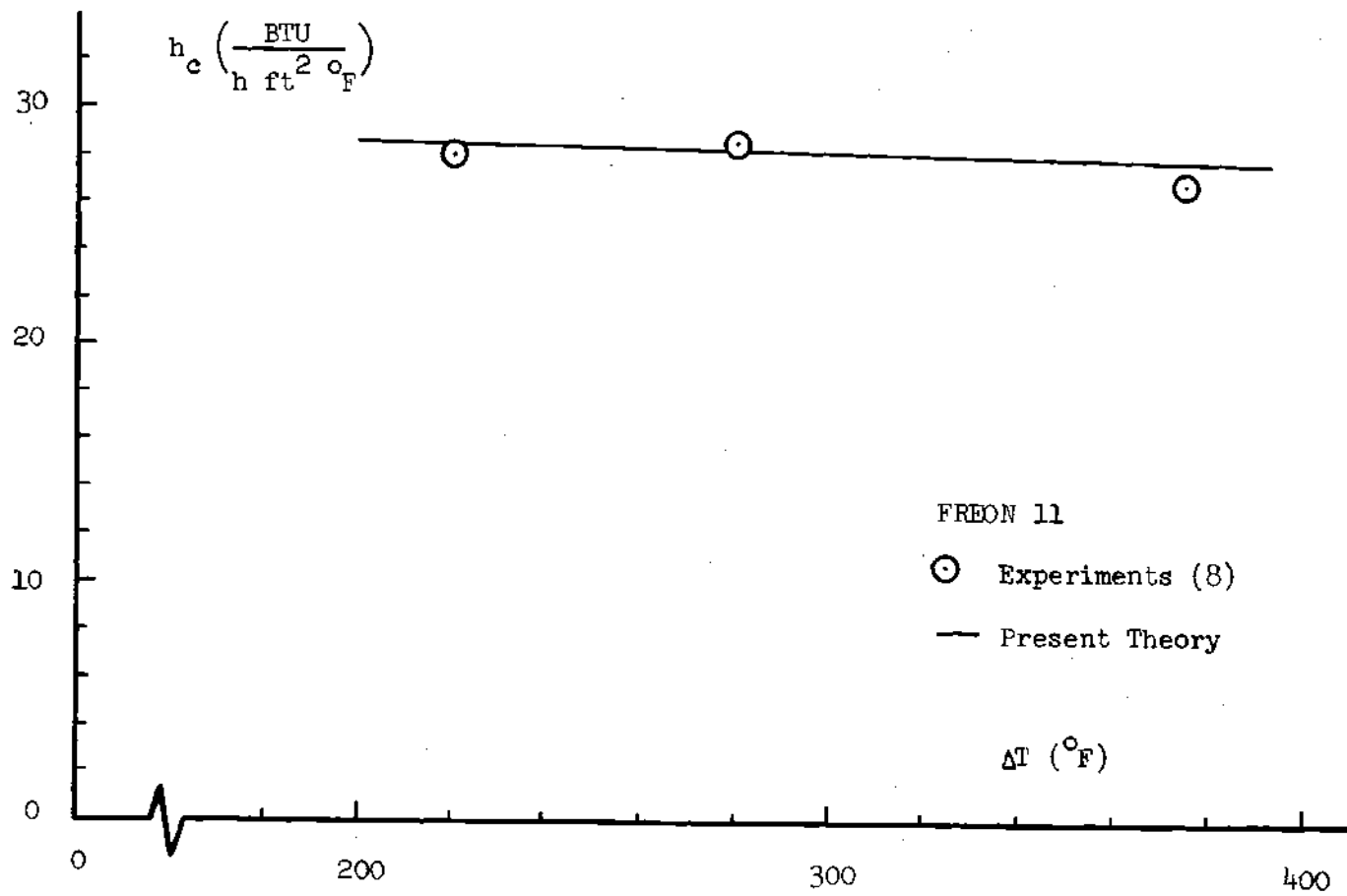


Figure 9. Heat Transfer Coefficient Versus Temperature Difference for Freon 11.

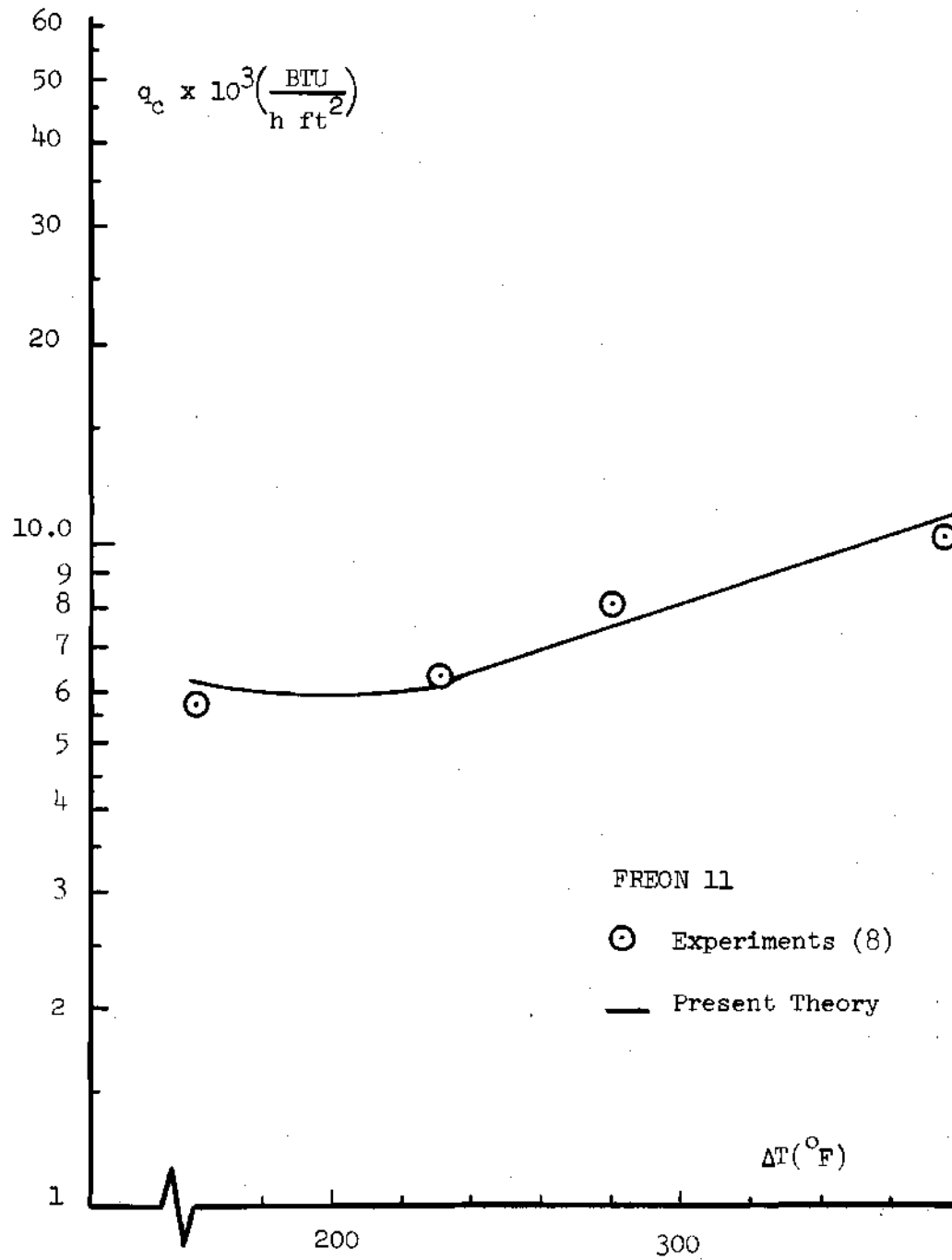


Figure 10. Heat Flux Versus Temperature Difference for Freon 11.

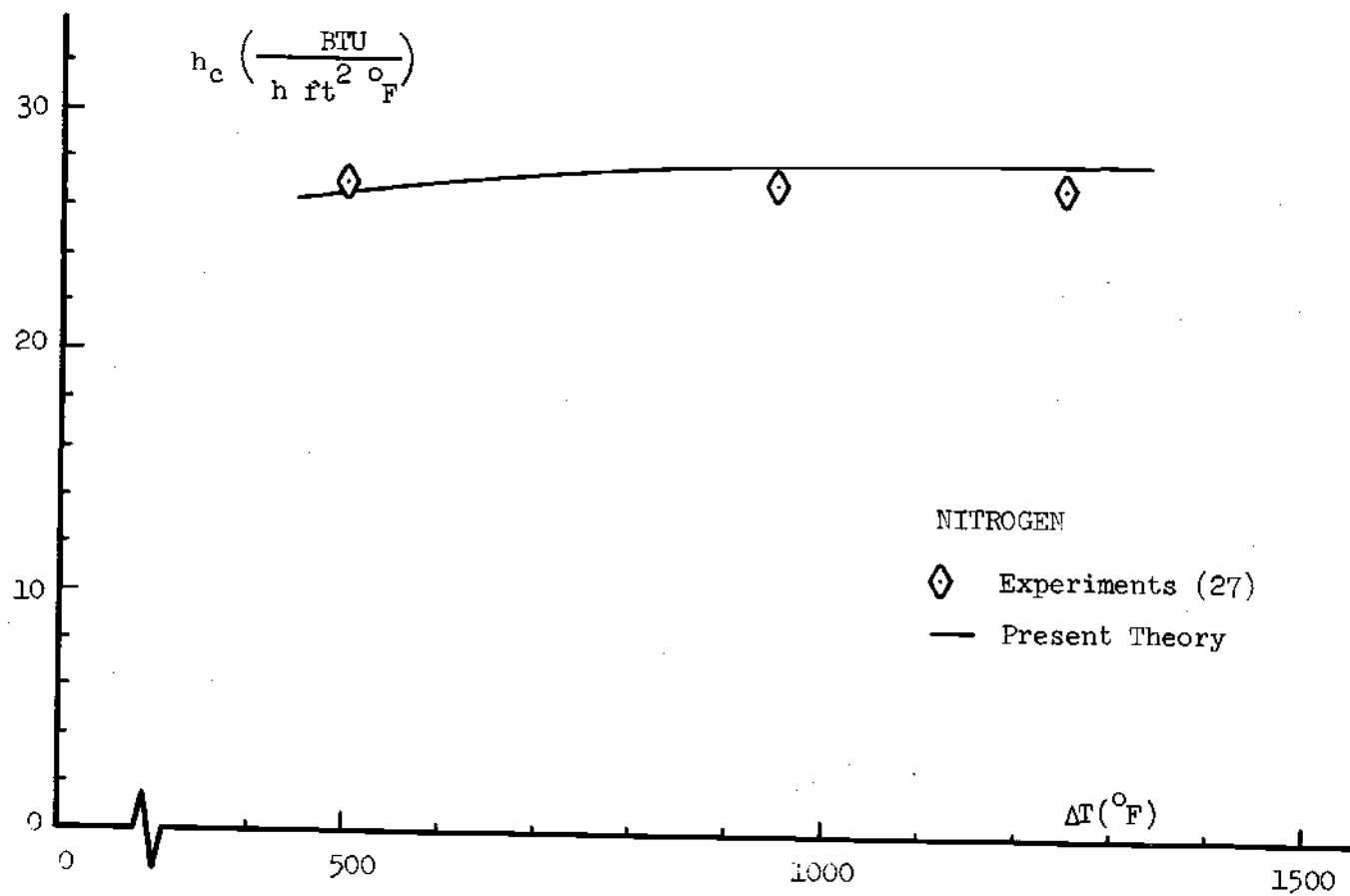


Figure 11. Heat Transfer Coefficient Versus Temperature Difference for Nitrogen.

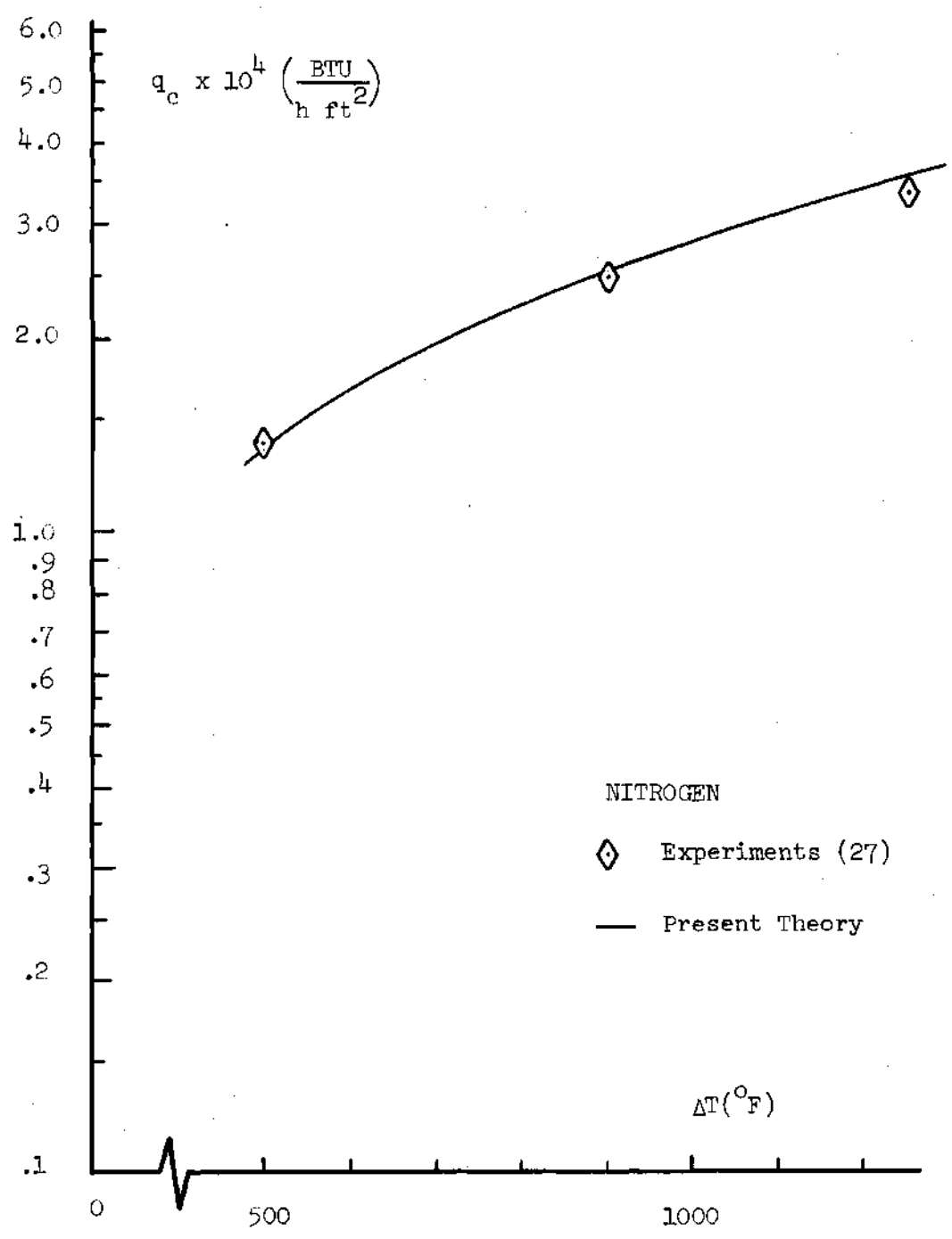


Figure 12. Heat Flux Versus Temperature Difference for Nitrogen.

CHAPTER VI

CONCLUSION

Pool film boiling from a flat horizontal surface has been studied analytically and the results are in good agreement with the experimental data available in the literature.

In a three-dimensional model, the wave velocity at the interface between two heated superposed fluids of finite depths has been first derived and is given by equation (37).

The analysis of the interface stability is then applied to the minimum heat flux and the film boiling region. In contrast to gravity, the mass transfer and the surface tension appear to have a stabilizing influence.

The three-dimensional treatment of the problem is more adequate than the usual two-dimensional approach to predict the flow pattern:

(a) the average interbubble distance varies between two values: the critical and most dangerous wavelengths given by equations (44) and (52) where the effect of the interfacial mass transfer appears explicitly.

(b) the average bubble diameter at breakoff is $1/\sqrt{2}$ times that distance

(c) the bubble diameter and the frequency of bubble release given by equation (60) agree very closely with the experimental measurements from a flat surface.

At high pressures, the modification of the boiling pattern can now be predicted theoretically. The change from a regularly bubbling interface to a large vapor sheet covering the heated surface happens when the non-dimensional term M_q , which scales the mass transfer and the gravity effects, equals unity.

At low pressure, however, for most of the fluids, the M_q term approaches unity only at extremely high values of the heat flux; and, therefore, the film boiling pattern keeps its rather regular characteristics up to very high temperature differences. This explains why the insertion of the mass transfer in the equation giving the minimum heat flux, that is, equation (63) brings little change in the actual value in comparison with the traditional relationships presented in the literature. The same holds to a smaller extent for the film boiling heat transfer coefficient whose expression, as given in equation (89), is also significantly influenced by the interfacial mass transfer only at very high temperatures.

Finally, a recommendation for further investigations can be proposed and this involves the carrying out of experiments of film boiling on a large flat horizontal surface at low pressures and high heat fluxes as well as at high pressures.

BIBLIOGRAPHY

1. Grigull, U. and Abadzic, E., "Blasen - und Filmsieden von Kohlendioxyd im kritischen Gebiet," Forsch. Ing. Wes., 31, N. 1, 1965, pp. 27-30.
2. Abadzic, E. and Goldstein, R. J., "Film Boiling and Free Convection Heat Transfer to Carbon Dioxide Near the Critical State," Int. J. Heat and Mass Transfer, Vol. 13, 1970, pp. 1163-1175.
3. Zuber, N., "Hydrodynamic Aspects of Boiling Heat Transfer," Ph.D. Thesis, Dept. of Eng., U.C.L.A., 1959.
4. Berenson, P. J., "Transition Boiling Heat Transfer from a Horizontal Surface," Technical Report No. 17, M.I.T., 1960.
5. Rankin, S., "Forced Convection Film Boiling Inside of Vertical Pipes," University of Delaware, Ph.D. Thesis, 1961.
6. Staub, F. W., and Zuber, N., "A Program of Two-Phase Flow Investigation," Second Quarterly Report, July-September 1963, U. S. Atomic Energy Commission Contract AT(04-3)-189, Project Agreement 35, EURAEC, GEAP 4367.
7. Hsieh, D. Y., "Effects of Heat and Mass Transfer on Rayleigh-Taylor Instability," ASME Transactions, March 1972, pp. 156-162.
8. Hosler, E. R., and Westwater, J. W., "Film Boiling on a Horizontal Plate," ARS Journal, April 1962, pp. 553-558.
9. Lamb, H., Hydrodynamics, Dover Publications, N. Y., 1945.
10. Maxwell, J. C., The Scientific Papers of James Clerk Maxwell, Vol. II, Dover Publications, N.Y., 1890.
11. Kocamustafaogullari, G., "Thermo-Fluid Dynamics of Separated Two-Phase Flow," Ph.D. Thesis, Georgia Institute of Technology, December 1971.
12. Chandrasekhar, S., Hydrodynamic and Hydromagnetic Stability, Oxford Clarendon Press, 1961.
13. Milne-Thompson, L. M., Theoretical Hydrodynamics, The Macmillan Company, N. Y., 1950.

14. Zuber, N., and Dougherty, D., "Fluid Dynamics of Dispersed Two-Phase Vapor-Liquid Flow in Lubricant Film," U. S. Atomic Energy Report, M.T.I. - 68-TR30, 1968.
15. Westwater, J. W., and Santangelo, J. G., "Photographic Study of Boiling," Ind. and Eng. Chemistry, Vol. 47, No. 8, August 1955, pp. 1605-1610.
16. Nishikawa, K., "Photographic Study of Saturated Free Convection Stable Film Boiling," Japanese Society of Mech. Eng., Vol. 4, No. 13, 1961, pp. 115-123.
17. Hosler, E. R., "Film Boiling on Horizontal Plates," Ph.D. Thesis, University of Illinois, 1961.
18. Bankoff, S. G., "On Taylor Instability of Plane Surfaces," Physics of Fluids, Vol. 2, 1959, pp. 576.
19. Kesselring, R. C., Rosche, P. H., Bankoff, S. G., "Transition and Film Boiling from Horizontal Strips," A.I.Ch.E. Journal, Vol. 13, No. 4, July 1967, pp. 669-675.
20. Kiper, A. M., "Maximum Bubble Departure Size in Pool Film Boiling," Proceedings of the Sixth Southeastern Seminar on Thermal Sciences, April 13-14, 1970, Raleigh, N. C., pp. 43-54.
21. Lienhard, J. H., and Wong, P. T. Y., "The Dominant Unstable Wavelength and Minimum Heat Flux During Film Boiling on a Horizontal Cylinder," Journal of Heat Transfer, ASME Transactions, Series C., Vol. 86, No. 2, 1964.
22. Lewis, D. J., "The Instability of Liquid Surfaces when Accelerated in a Direction Perpendicular to Their Plane," Proceedings of the Royal Society, London, Vol. 202, 1950.
23. Zuber, N., "On the Stability of Boiling Heat Transfer," ASME Transactions, Vol. 80, April 1958, pp. 711-720.
24. Berenson, P. J., "Film Boiling Heat Transfer from a Horizontal Surface," ASME Paper No. 60-WA-147, 1960.
25. Jakob, M., Heat Transfer, Vol. II, John Wiley and Sons, N. Y., 1957.
26. Bromley, L. A., "Heat Transfer in Stable Film Boiling," Ph.D. Thesis, University of California, Berkeley, 1948.
27. Sauer, H. J., Jr., and Ragsdell, K. M., "Film Pool Boiling of Nitrogen from Flat Surfaces," Advances in Cryogenic Engineering, Vol. 16, 1971, pp. 412-415.